ChemComm

Dye-sensitized photocatalytic hydrogen production: enhanced activity in a glucose derivative of a phenothiazine dye

Journal:	*ChemComm*
Manuscript ID	Draft
Article Type:	Communication
Date Submitted by the Author:	n/a

Complete List of Authors:	Manfredi, Norberto; University of Milano-Bicocca, Materials Science Department - MIB-Solar Cecconi, Bianca; University of Milano-Bicocca, Materials Science Department - MIB-Solar Calabrese, Valentina; Università degli Studi Milano-Bicocca, Biotechnology and Biosciences Minotti, Alberto; Universita degli Studi di Milano-Bicocca, Biotechnology and Biosciences Peri, Francesco; University of Milano-Bicocca, Biotechnology and Biosciences Ruffo, Riccardo; University of Milano-Bicocca, Materials Science Department - MIB-Solar Monai, Matteo; University of Trieste, Dipartimento di Scienze Chimiche Romero-Ocaña, Ismael; University of Trieste, Dipartimento di Scienze Chimiche Montini, Tiziano; University of Trieste, Dipartimento di Scienze Chimiche Fornasiero, P; Univ. degli Studi di Trieste, Dipartimento di Scienze Chimiche Abbotto, Alessandro; University of Milano-Bicocca, Materials Science Department - MIB-Solar

University of Milano-Bicocca

Via R. Cozzi 55, I-20125 Milano, Italy
http://www.mater.unimib.it

Milano, 15 January 2016

Chemical Communications
The Editor

Dear Editor,

Please find herewith enclosed the manuscript:

"Dye-sensitized photocatalytic hydrogen production: enhanced activity in a glucose derivative of a phenothiazine dye"

by N. Manfredi, B. Cecconi, V. Calabrese, A. Minotti, F. Peri, R. Ruffo, M. Monai, I. Romero-Ocaña, T. Montini, P. Fornasiero and A. Abbotto

that we would like to submit to *ChemComm* for publication as a Communication.

This work introduces a new concept for the design of organic photosensitizers for the photocatalytic production of hydrogen from water and sunlight. In this field a rational design of sensitizers is urgently required to improve performances and stability of the photocatalytic system. Here we prove the concept of enhancing the photocatalytic hydrogen production rate by optimizing the wettability of a dye-sensitized TiO_2 nanoparticles photocatalyst. With this goal in mind, we specifically modified a phenothiazine scaffold as a sensitizer, that we have recently applied with success to the photocatalytic hydrogen generation (B. Cecconi, N. Manfredi, R. Ruffo, T. Montini, I. Romero-Ocaña, P. Fornasiero and A. Abbotto, *ChemSusChem*, 2015, **8**, 4216), by introducing a glucose functionality (**PTZ-GLU**) to guarantee improved affinity for water. This work clearly demonstrated that, while keeping unvaried the aromatic π-conjugated framework necessary for the sensitization of the phocatalyst, the enhanced wettability of the **PTZ-GLU** derivative significantly boosts the photocatalytic performances both of evolved hydrogen and turnover number. Taking into account that the derivatization procedure uses a simple and up-scalable synthetic procedure we strongly believe that these innovative results pave the way to the design of a new family of efficient sensitizers for dye-sensitized photocatalytic hydrogen generation.

Considering the potential general implications of the proposed novel strategies for the design of more efficient dyes sensitizers in various rapidly growing sectors of research (artificial photosynthesis and solar fuels) we believe that the work meets the criteria of high quality and urgency of ChemComm. Looking forward to having the opportunity to receive inputs from referees. Thank you very much for your consideration.

Best regards,

Alessandro Abbotto and Paolo Fornasiero

Journal Name

COMMUNICATION

Dye-sensitized photocatalytic hydrogen production: enhanced activity in a glucose derivative of a phenothiazine dye

Received 00th January 20xx,
Accepted 00th January 20xx

DOI: 10.1039/x0xx00000x

www.rsc.org/

N. Manfredi,[a] B. Cecconi,[a] V. Calabrese,[b] A. Minotti,[b] F. Peri,[b] R. Ruffo,[a] M. Monai,[c] I. Romero-Ocaña,[c] T. Montini,[c] P. Fornasiero*[c] and A. Abbotto[a]*

A thiophene-based donor-acceptor phenothiazine dye has been functionalized with a peripheral glucose unit (PTZ-GLU) to bust its affinity to water and enhance dye-sensitized photogeneration of hydrogen. Compared to the common hydrophilic triethylene glycol substitution (PTZ-TEG), the sugar derivative shows a lower contact angle and a generation of hydrogen twice more efficient in terms of evolved gas and turnover number.

The role of hydrogen as a clean and sustainable energy vector is recently attracting a growing interest in the scientific and technological community.[1] Photocatalysis is the ideal way to generate hydrogen from water simply using a suitable catalytic system and sunlight. Unfortunately, despite great efforts in the last decades,[2] the overall efficiencies are still far from being economically viable for real applications.[1b] Homogeneous systems,[3] pure[4] and nanocomposites semiconductors[2c] have been widely investigated. In this context, dye-sensitization has recently emerged as a promising alternative to enhance photocatalytic efficiency by exploiting the visible range of the solar irradiation.[5] At the present time, rational design of dye-sensitizers is therefore urgently required to improve performances and stability of the photocatalytic system. We have recently described a series of new donor-acceptor phenothiazine (PTZ) sensitizers containing thiophene-based spacers, showing that a careful design of the thiophene unit can afford improved long-term H_2 production rates and enhanced sensitizer stability under irradiation.[6] The photocatalytic system comprised a two-component scheme where the dye-sensitizer is associated to a redox storing catalyst such as Pt/TiO_2. The PTZ series was characterized by the presence of a terminal alkyl substituent providing an hydrophobic nature to the sensitizers, which is not optimal for affinity to the aqueous working conditions.[6]

In this paper we prove the concept of improving the photocatalytic hydrogen production rate from aqueous solutions by enhancing the wettability of a dye-sensitized TiO_2 nanoparticles (TiO_2-NP) photocatalyst. One of the most common strategies to induce hydrophilicity to organic dyes is the introduction of a polyethylene glycol functionality, such as the widely used tris(ethylene glycol) monomethyl ether (TEG) group.[7] In fact, the TEG group has been successfully employed in many material science fields, including dye-sensitized solar cells[8] and nonlinear optics.[9] More recently, the use of poly-glycolic functionalities as substituents in organic molecules for dye-sensitized hydrogen generation has been also reported.[5e] Despite these several reports, the TEG functionality cannot imply a more sophisticated design to further tune water affinity of sensitizers or induce additional properties such as intermolecular self-assembling. We have thus decided to check the use of a multifunctional scaffold derived from the natural monosaccharide D-glucose. Carbohydrates are excellent hydrogen bond donors and acceptors thanks to their multiple hydroxyl functions; sugar conjugation to hydrophobic molecular materials has been used in other research fields to enhance wettability.[10] D-glucose derivatives have been recently used in material science to induce self-aggregation.[11]

Here we report on the synthesis, characterization and comparative use of a TEG (**PTZ-TEG**) and sugar (**PTZ-GLU**) derivative of a thiophene-based phenothiazine dye (Fig. 1) belonging to the aforementioned PTZ family. In order to similarly compare with the small TEG substituent, we have

[a] *Department of Materials Science and Solar Energy Research Center MIB-SOLAR, University of Milano-Bicocca, and INSTM Milano-Bicocca Research Unit, Via Cozzi 55, I-20125, Milano, Italy*
[b] *Department of Biotechnology and Biosciences, University of Milano-Bicocca, Piazza della Scienza, 2, 20126 Milano, Italy*
[c] *Department of Chemical and Pharmaceutical Sciences and ICCOM CNR Trieste Research Unit, University of Trieste, via L. Giorgieri 1, I-34127, Trieste, Italy*
† Footnotes relating to the title and/or authors should appear here.
Electronic Supplementary Information (ESI) available: [synthetic schemes and experimental procedures, optical and electrochemical characterization, optimization procedures for H_2 measurements, ^{1}H-NMR and ^{13}C-NMR]. See DOI: 10.1039/x0xx00000x

selected the commercially available methyl α-D-glucopyranoside moiety. We demonstrate that the unprecedented use of the sugar functionalization in this field is able to significantly improve the wettability of the TiO_2 materials sensitized with the new PTZ derivatives and enhance the sunlight-driven hydrogen generation compared to its TEG counterpart both in terms of evolved gas and turnover number (TON).

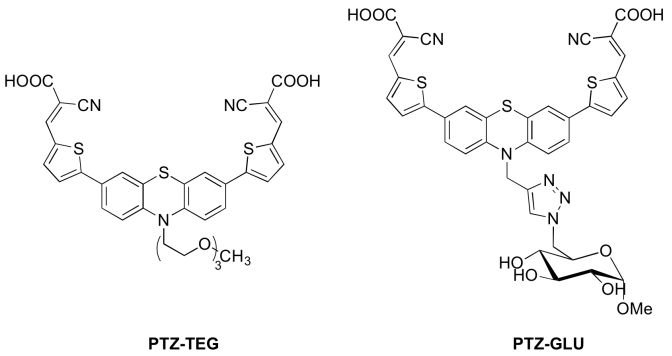

Figure 1: Target hydrophilic sensitizers investigated in this work.

In order to modify the wettability properties of the dye:catalyst surface without interfering with the conjugated π skeleton of the sensitizer, which is responsible for the light harvesting step of the photocatalytic process, we introduced the hydrophilic groups on the terminal electron-rich (donor) core of PTZ by exploiting the nitrogen site of the heterocyclic ring. The two groups were spaced by a methylene linker to block communication with the π system. In this way we did not induce any modification of on the π-conjugated system and could relate the effect of the two terminal groups, in terms of dye wettability, to the hydrogen generation. The sugar functionality of **PTZ-GLU** has been introduced by exploiting click chemistry and Cu-assisted azide-alkyne Huisgen cycloaddition.[12] Although alternative synthetic paths could be envisaged, we selected the click chemistry approach in order to ensure design flexibility, extension to a library of glycoconjugated dyes,[13] and complete transfer to the industrial scale. The sugar is in form of α-methyl glucopyranoside in order to prevent any possible redox interference of the anomeric free aldehyde with the photocatalytic cycle of the sensitizer. The synthetic access to **PTZ-TEG** and **PTZ-GLU** is illustrated in Scheme S1 and detailed experimental procedure is described in ESI.

Absorption spectra of dyes **PTZ-TEG** and **PTZ-GLU** (10^{-5} M in THF) are shown in Fig. S1 (ESI) and main optical and energetic (HOMO-LUMO energies) parameters are listed in Table S1 (ESI). As expected, optical properties of the two dyes were not affected by the presence of the two different hydrophilic substituents. Both dyes showed a typical behaviour with an intense π-π* absorption band in the Vis region attributed to the intramolecular charge-transfer transition. The position of the absorption maximum is ca. 470 nm for both dyes whereas peak molar absorptivity is slightly different though very similar (ca. 10% deviation). The electrochemical characterization is summarized in Figs. S2 and S3 (ESI) and Table S1 (ESI). Cyclic voltammetry profiles showed a quasi-reversible behaviour for the **PTZ-TEG** oxidation. The remaining investigated redox processes (**PTZ-TEG** reduction and **PTZ-GLU** oxidation and reductions) were irreversible. The **PTZ-TEG** oxidation showed two unresolved current signals (a peak and its shoulder), which made somewhat difficult the energy level calculation. For these reasons, Differential Pulsed Voltammetry (DPV) was employed. DPV was able to isolate the different electrochemical processes with the exception of the **PTZ-GLU** first oxidation, which appears as a shoulder of the main peak. In this case the HOMO energy level has been determined from the current onset rather than current peak.

Contact angle analysis was used to investigate the hydrophilicity properties of the **PTZ-TEG** and **PTZ-GLU** sensitized TiO_2 nanoparticles. The contact angles of a deionized water drop on the surface of a film of sintered TiO_2 and the corresponding films sensitized with both dyes are shown in Figure 2; data are summarized in Table 1. The bare TiO_2 and the dyes-sensitized films have contact angles lower than 35°. More importantly, the sugar functionality in **PTZ-GLU** is able to improve water affinity by decreasing the angle from 34° in the **PTZ-TEG** dye to 27°, going closer to the bare TiO_2-NP surface character.

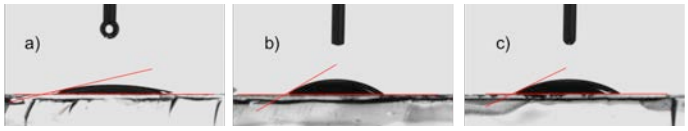

Figure 2: Cross-sections of a) a film of sintered TiO_2-NP; b) film of sintered TiO_2-NP sensitized with **PTZ-TEG**; c: film of sintered TiO_2-NP sensitized with **PTZ-GLU** and a drop of deionized water positioned on the top, which were used for the estimation of the contact angles (ϑc/°).

Table 1: Contact angle and photocatalytic performance of the dye/Pt/TiO_2 materials in H_2 production from TEOA 10% v/v solution at pH = 7.0 under irradiation with visible light (λ > 420 nm).

Sample	Dye loading (μmol g^{-1})	Contact angle (ϑc/°)	H_2 amount [a] (μmol g^{-1})	TON [b]	LFE_{20} [c]
TiO_2-NP	-	13.86	-	-	-
PTZ-TEG	30.0	33.86	421	14.4	0.012
PTZ-GLU	30.1	26.80	862	29.6	0.027

[a] Overall H_2 amount produced after 20 h of irradiation; [b] TON = (2 x H_2 amount)/(dye loading); [c] Light-to-Fuel Efficiency calculated after 20 h of irradiation.

Pt/TiO_2 has been used as benchmark material to test the comparative sensitization ability of the new dyes under irradiation with visible light (λ > 420 nm). The Pt/TiO_2 material (Pt loading of 1 wt%) has been prepared by photodeposition of Pt nanoparticles on the surface of TiO_2 P25 using a EtOH/water solution of $Pt(NO_3)_2$. The Pt/TiO_2 material is an anatase/rutile mixture (~ 70/30 by weight)

with mean crystallite sizes of 20 nm for both phases. Textural analysis revealed a surface area of 55 m^2/g with pores diameters around 48 nm and a pore volume of 0.242 mL/g. HAADF-STEM analysis (Fig. 3) evidenced the irregular shape of TiO_2 particles (12 – 45 nm), with Pt nanoparticles with mean size of 2.4 nm homogenously distributed on the surface of the support.

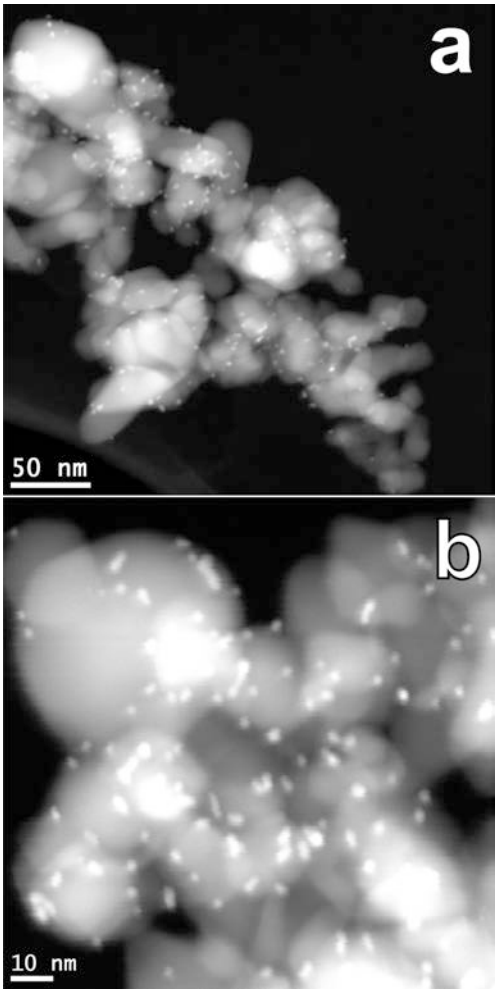

Figure 3: Representative HAADF-STEM images of the Pt/TiO_2 nanocomposite.

The **PTZ-TEG** and **PTZ-GLU** dyes have been adsorbed on Pt/TiO_2 nanocomposite by suspending the powder into an EtOH/DMSO solution of the dye in the dark for 12 h, in order to reach a loading of 30 μmol g^{-1}. After recovery of powder by filtration, the amount of residual dye in the solution was negligible, as assessed by UV-Vis spectroscopy. The Pt/TiO_2 photocatalysts sensitized by **PTZ-TEG** and **PTZ-GLU** were tested for H_2 production under Vis light (λ > 420 nm) from a triethanolamine (TEOA)/HCl aqueous buffer solution at pH = 7.0. Following the "best practice in photocatalysis" reported by Kisch and Bahnenmann,[14] the experimental conditions have been optimized measuring the H_2 production rate after stabilization (see below) using different amounts of the photocatalyst. This preliminary optimization has been performed using the **PTZ-GLU**/Pt/TiO_2 photocatalyst (Fig. S4). Maintaining constant all the other experimental factors (geometry of irradiation and reactor, volume of the TEOA/HCl solution, temperature, etc.), the maximum H_2 production rate has been obtained using 60 mg of the photocatalyst, with a slight decrease for higher amounts likely due to increased scattering of the incoming photons.

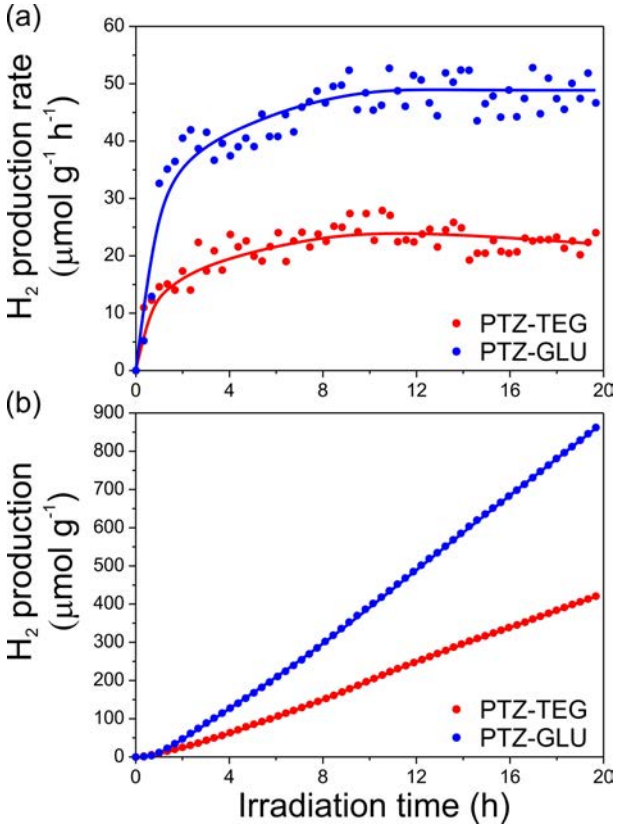

Figure 4 : Production rates (a) and overall productivities (b) in H_2 evolution from TEOA 10% v/v solution at pH = 7.0 under irradiation with visible light (λ > 420 nm) using the Pt/TiO_2 materials sensitized with **PTZ-TEG** and **PTZ-GLU**.

The H_2 production rates using **PTZ-TEG** and **PTZ-GLU** sensitized photocatalysts (Fig. 4a) showed an initial increase in the first 8 – 9 h under irradiation. This phenomenon arises from the combination of two factors. First, diffusion of produced H_2 in the dead volume of the photoreactor resulted in the progressive increase of H_2 concentration in the gaseous effluent for the system, which typically accounts for the first 1-2 h. Second, activation of the photocatalyst took place at the beginning of each photocatalytic experiment, likely because the Pt nanoparticles were passivated by the adsorbed oxygen resulting from exposure to air after photodeposition. This progressive activation of the photocatalysts resulted in an initial delay, as evident by plotting the amount of evolved gas (Fig. 4b). Notably, no H_2 production was observed using the bare Pt/TiO_2 under the same experimental conditions.
From these data we observe that the H_2 production rate of the **PTZ-GLU** sensitized photocatalyst is about twice that of the **PTZ-TEG** system. Accordingly, the TON value and the Light-to-Fuel Efficiency after 20 hours of irradiation

(LFE_{20}), listed in Table 1, have doubled in the case of the glucose derivative compared to the TEG dye.

In conclusion, this study has introduced for the first time in the field of the dye-sensitized photocatalytic production of hydrogen the use of sugar derivatives to optimize the catalyst design and improve the overall efficiency of hydrogen production. Using as a reference dye scaffold a multibranched derivative of phenothiazine, previously used with success, we demonstrated that the insertion of the glucose unit has allowed to improve the affinity towards the aqueous medium, in which the catalyst has to operate, compared to the common TEG functionality. This afforded, while maintaining unvaried the other properties associated to the π-conjugated system of the sensitizer, to double the efficiency of hydrogen production, both in terms of produced gas and TON. The used general and scalable synthetic approach and the available large variety of sugar derivatives will allow the access to a library of new photosensitizers with finely modulated properties and abilities to improve the efficiency of the production of solar fuels.

Acknowledgments

AA, BC, and NM thank the Ministero dell'Istruzione, Università e della Ricerca (MIUR-PRIN) (grant number 2008CSNZFR) for financial support. MM, IRO, TM and PF acknowledge the Ministero dell'Istruzione, Università e Ricerca (Project 2010N3T9M4 "HI-PHUTURE"), University of Trieste (FRA2013 Project).

Notes and references

1 (a) N. Armaroli and V. Balzani, in *Energy for a Sustainable World*, Wiley-VCH Verlag GmbH & Co. KGaA, 2010; (b) N.Armaroli and V. Balzani, *ChemSusChem*, 2011, **4**, 21; (c) N. Armaroli and V. Balzani, *Chem. Eur. J.*, 2016, **22**, 32.

2 (a) A. Fujishima and K. Honda, *Nature*, 1972, **238**, 37; (b) M. Cargnello, A. Gasparotto, V. Gombac, T. Montini, D. Barreca and P. Fornasiero, *Eur. J. Inorg. Chem.*, 2011, **2011**, 4309; (c) W. Fan, Q. Zhang and Y. Wang, *Phys. Chem. Chem. Phys.*, 2013, **15**, 2632; (d) M. K. Bhunia, K. Yamauchi and K. Takanabe, *Angew. Chem. Int. Ed.*, 2014, **53**, 11001; (e) T. A. Kandiel, D. H. Anjum and K. Takanabe, *ChemSusChem*, 2014, **7**, 3112.

3 (a) J. L. Dempsey, B. S. Brunschwig, J. R. Winkler and H. B. Gray, *Acc. Chem. Res.*, 2009, **42**, 1995; (b) P. Du, K. Knowles and R. Eisenberg, *J. Am. Chem. Soc.*, 2008, **130**, 12576; (c) S. Losse, J. G. Vos and S. Rau, *Coord. Chem. Rev.*, 2010, **254**, 2492; (d) T. M. McCormick, B. D. Calitree, A. Orchard, N. D. Kraut, F. V. Bright, M. R. Detty and R. Eisenberg, *J. Am. Chem. Soc.*, 2010, **132**, 15480.

4 X. Chen, S. Shen, L. Guo and S. S. Mao, *Chem. Rev.*, 2010, **110**, 6503.

5 (a) R. Abe, K. Shinmei, N. Koumura, K. Hara and B. Ohtani, *J. Am. Chem. Soc.*, 2013, **135**, 16872; (b) L. Andrade, R. Cruz, H. A. Ribeiro and A. Mendes, *Int. J. Hydrogen Energy*, 2010, **35**, 8876; (c) W.-S. Han, K.-R. Wee, H.-Y. Kim, C. Pac, Y. Nabetani, D. Yamamoto, T. Shimada, H. Inoue, H. Choi, K. Cho and S. O. Kang, *Chem. Eur. J.*, 2012, **18**, 15368; (d) J. Lee, J. Kwak, K. C. Ko, J. H. Park, J. H. Ko, N. Park, E. Kim, D. H. Ryu, T. K. Ahn, J. Y. Lee and S. U. Son, *Chem. Comm.*, 2012, **48**, 11431; (e) S.-H. Lee, Y. Park, K.-R. Wee, H.-J. Son, D. W. Cho, C. Pac, W. Choi and S. O. Kang, *Org. Lett.*, 2010, **12**, 460; (f) X. Li, S. Cui, D. Wang, Y. Zhou, H. Zhou, Y. Hu, J.-g. Liu, Y. Long, W. Wu, J. Hua and H. Tian, *ChemSusChem*, 2014, **7**, 2879; (g) M. Watanabe, H. Hagiwara, A. Iribe, Y. Ogata, K. Shiomi, A. Staykov, S. Ida, K. Tanaka and T. Ishihara, *J. Mater. Chem. A*, 2014, **2**, 12952.

6 B. Cecconi, N. Manfredi, R. Ruffo, T. Montini, I. Romero-Ocaña, P. Fornasiero and A. Abbotto, *ChemSusChem*, 2015, **8**, 4216.

7 R. Y.-Y. Lin, F.-L. Wu, C.-T. Li, P.-Y. Chen, K.-C. Ho and J. T. Lin, *ChemSusChem*, 2015, **8**, 2503.

8 V. Leandri, H. Ellis, E. Gabrielsson, L. Sun, G. Boschloo and A. Hagfeldt, *Phys. Chem. Chem. Phys.*, 2014, **16**, 19964.

9 L. Berti, M. Cucini, F. Di Stasio, D. Comoretto, M. Galli, F. Marabelli, N. Manfredi, C. Marinzi and A. Abbotto, *J. Phys. Chem. C*, 2010, **114**, 2403.

10 R. Narain, *Engineered Carbohydrate-Based Materials for Biomedical Applications*, John Wiley & Sons, Inc., 2011.

11 G. Pescitelli, O. H. Omar, A. Operamolla, G. M. Farinola and L. Di Bari, *Macromolecules*, 2012, **45**, 9626.

12 (a) Y. M. Chabre and R. Roy, *Chem. Soc. Rev.*, 2013, **42**, 4657; (b) E. Haldon, M. C. Nicasio and P. J. Perez, *Org. Biom. Chem.*, 2015, **13**, 9528.

13 C. W. Tornøe, C. Christensen and M. Meldal, *J. Org. Chem.*, 2002, **67**, 3057.

14 H. Kisch and D. Bahnemann, *J. Phys. Chem. Lett.*, 2015, **6**, 1907.

Dye-sensitized photocatalytic hydrogen production: enhanced activity in a glucose derivative of a phenothiazine dye

By N. Manfredi, B. Cecconi, V. Calabrese, A. Minotti, F. Peri, R. Ruffo, M. Monai, I. Romero-Ocaña, T. Montini, P. Fornasiero* and A. Abbotto*

Electronic Supplementary Information (ESI)

Experimental Section

General information

NMR spectra were recorded with a Bruker AMX-500 spectrometer operating at 500.13 MHz (^{1}H) and 125.77 MHz (^{13}C). Coupling constants are given in Hz. Absorption spectra were recorded with a V-570 Jasco spectrophotometer. Flash chromatography was performed with Merck grade 9385 silica gel 230–400 mesh (60 Å). Reactions performed under inert atmosphere were done in oven-dried glassware and a nitrogen atmosphere was generated with Schlenk technique. Conversion was monitored by thin-layer chromatography by using UV light (254 and 365 nm) as a visualizing agent. All reagents were obtained from commercial suppliers at the highest purity grade and used without further purification. Anhydrous solvents were purchased from Sigma-Aldrich and used without further purification. Extracts were dried with Na_2SO_4 and filtered before removal of the solvent by evaporation.

Electrochemical characterization

Test solutions were prepared by dissolving 2.3 and 2.2 mg of PTZ-TEG and PTZ-GLU, respectively, in the electrolyte (0.1 M $TBAClO_4$ in DMSO). DPV and CV were carried out at scan rate of 20 and 50 mV/s, respectively, using a PARSTA2273 potentiostat in a two-compartment, 3-electrode electrochemical cell in a glove box filled with N_2 ($[O_2]$ and $[H_2O] \leq 0.1$ ppm). The working, counter, and the pseudo-reference electrodes were a glassy carbon pin, a Pt flag and an Ag/AgCl wire, respectively. The working electrodes discs were well polished with alumina 0.1 μm suspension, sonicated for 15 min in deionized water, washed with 2-propanol, and cycled for 50 times in 0.5 M H_2SO_4 before use. The Ag/AgCl pseudo-reference electrode was calibrated, by adding ferrocene (10^{-4} M) to the test solution after each measurement. Energy levels were calculated using the absolute value of 5.2 V vs. vacuum for the ferrocene reference couple.

Preparation of Pt/TiO_2 nanocomposite

Deposition of Pt nanoparticles on TiO_2 Degussa P25 was done through a photodeposition method known in literature.[1-4] 32.7 mg of $Pt(NO_3)_2$ was dissolved in 400 mL of a solution of water/ethanol 1:1 by volume. 2.0 g of TiO_2 Degussa P25 was suspended in the Pt solution in order to reach a final metal loading of 1.0 wt%. After stirring for 1 h in the dark, the suspension was irradiated with a 450 W medium pressure lamp for 4 h. The Pt/TiO_2 nanocomposites were collected by centrifugation, washed 3 times with EtOH and finally dried under vacuum at 50 °C overnight.

Characterization of Pt/TiO_2 nanocomposite

Phase composition has been determined by Powder X-ray Diffraction (PXRD) using a Philips X'Pert diffractometer using a Cu Kα ($\lambda = 0.154$ nm) X-ray source in the range $10° < 2\theta < 100°$ and data were analyzed by using the PowderCell 2.0 software. Mean crystallite sizes were calculated applying the Scherrer's equation to the principal reflection of each phase [(101) for anatase and (110) for rutile].

Textural properties of the catalyst have been analyzed by N_2 physisorption at the liquid nitrogen temperature using a Micromeritics ASAP 2020 automatic analyzer. The samples were previously degassed under vacuum at 200°C overnight. Specific surface area has been determined applying the BET method to the adsorption isotherm in the range $0.10 < p/p^0 < 0.35$. Pore size distribution has been evaluated applying the BJH theory to the desorption branch of the isotherm.[5]

The morphology of the composite materials and the distribution of the supported Pt nanoparticles were evaluated by High Resolution Transmission Electron Microscopy (HR-TEM) and High Angle Annular Dark Field-Scanning Transmission Electron Microscopy (HAADF-STEM) images recorded by a JEOL 2010-FEG microscope operating at the acceleration voltage of 200 kV. The microscope has 0.19 nm spatial resolution at Scherzer defocus conditions in HR-TEM mode and a probe of 0.5 nm was used in HAADF-STEM mode.

Adsorption of dyes on Pt/TiO_2

200 mg of Pt/TiO_2 nanocomposite were suspended in 10 mL of dye solution (0.3 mM in ethanol) for 24 h in the dark. The obtained materials were recovered by centrifugation, washed 2 times with 10

mL of EtOH each and dried under vacuum at room temperature overnight. UV-vis spectra of the solutions after dye adsorption showed that the amount of residual dyes is negligible, confirming the quantitative adsorption of the dyes on Pt/TiO_2.

Photocatalytic hydrogen production

The **PTZ-TEG**/Pt/TiO_2 and **PTZ-GLU**/Pt/TiO_2 nanomaterials have been tested for H_2 production following a procedure previously described.[6] The required amount of the photocatalyst was suspended into 60 mL of 10% v/v aqueous solution of triethanolamine (TEOA) previously neutralized with HCl. After purging with Ar (15 mL min^{-1}) for 30 min, the suspension was irradiated using a 150 W Xe lamp with a cut-off filter at 420 nm. Irradiance was ~ 6 x 10^{-3} W m^{-2} in the UV-A range and ~ 1080 W m^{-2} in the visible range (400 – 1000 nm). The concentration of H_2 in gas stream coming from the reactor has been quantified using a Agilent 7890 gaschromatograph equipped with a TCD detector, connected to a Carboxen 1010 column (Supelco, 30 m x 0.53 mm ID, 30 µm film) using Ar as carrier. Notably, the amount of catalyst has been optimized following the indications recently presented by Kisch and Bahnenmann.[7] The optimization has been performed using the **PTZ-GLU**/Pt/TiO_2 photocatalyst, increasing the amount of catalyst employed until the optimal H_2 production rate has been obtained (further addition of catalyst did not afford increased production of H_2). The optimum amount of photocatalyst has been found to be 60 mg as illustrated in Figure S4.

The performances of the sensitized photocatalysts have been reported in terms of H_2 production rate and overall H_2 productivity. Turn-Over Numbers (TON) were calculated as (2 x overall H_2 amount) / (dye loading). Light-to-Fuel Efficiency (LFE) was calculated as:

$$LFE = \frac{F_{H_2} * \Delta H^0_{H_2}}{S * A_{irr}}$$

where F_{H2} is the flow of H_2 produced (expressed in mol s^{-1}), ΔH^0_{H2} is the enthalpy associated with H_2 combustion (285.8 kJ mol^{-1}), S is the total incident light irradiance, as measured by adequate radiometers in 400 – 1000 nm ranges (expressed in W cm^{-2}) and A_{irr} is the irradiated area (expressed in cm^2).

UV-vis spectra of the aqueous solutions recovered at the end of the photocatalytic runs highlighted that no desorption of the dyes took place during the experiments.

Scheme S1: Synthesis of PTZ-TEG and PTZ-GLU.

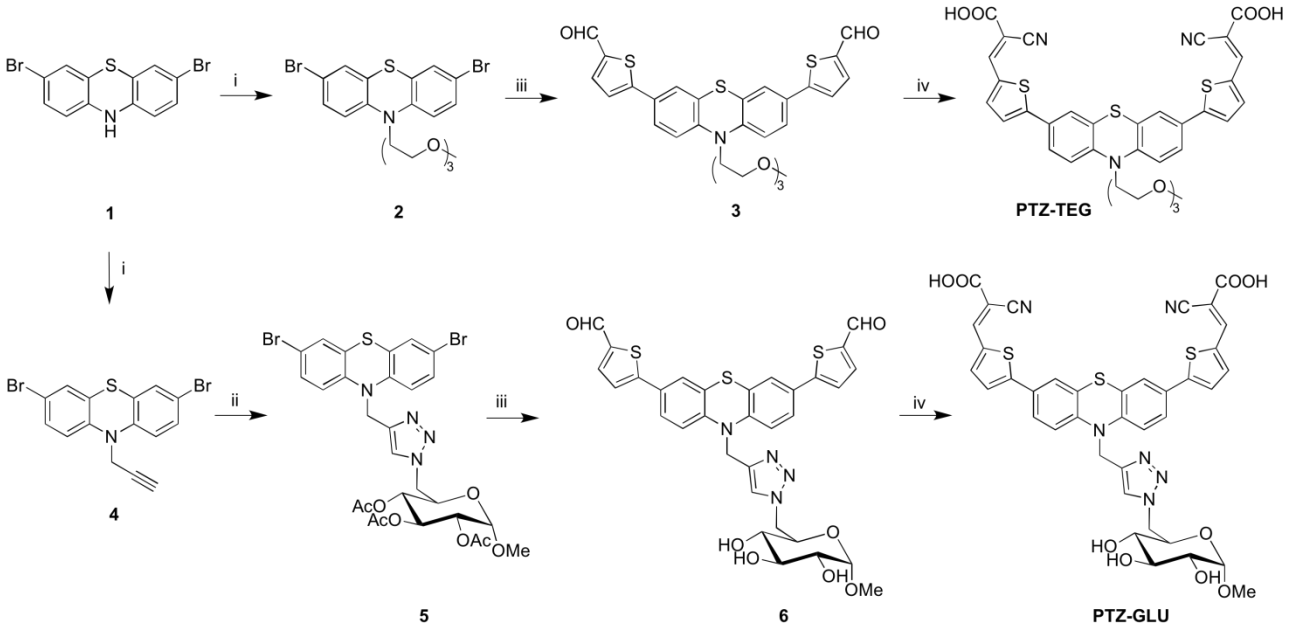

Reagents and conditions: (i) a. NaH 60%, DMF, 0°C, b. TEG-OTs for **2** and propargyl bromide for **4**, rt, 4 h; (ii) methyl 2,3,4-tri-*O*-acetyl-6-azido-6-deoxy-α-D-glucopyranoside, $Cu_2SO_4 \cdot 5H_2O$,

sodium ascorbate, THF/H_2O, rt, 4 h; (iii) 5-formyl-2-thienylboronic acid, Pd(dppf)Cl_2·CH_2Cl_2 [dppf = 1,1′-bis(diphenylphosphino)ferrocene], K_2CO_3, DME/MeOH, microwave, 70 °C, 90 min; (iv) cyanoacetic acid, piperidine, $CHCl_3$, reflux, 5 h.

The synthetic procedure for achieving **PTZ-TEG** is similar to the one used for **PTZ2**,[6] the alkylating reagent was prepared according to a known procedure starting from triethylene glycol monomethyl ether and *p*-TsOH.[8] Phenothiazine was brominated with Br_2 following the reported procedure,[9] then the anilinic nitrogen was deprotonated with NaH 60% in DMF followed by addition of the prepared tosylate. A following Suzuki-Miyaura cross coupling to introduce the π portion and a Knoevenagel condensation to introduce the anchoring and accepting unit enabled to afford **PTZ-TEG** with satisfactory yields.[6]

To obtain the glucose-functionalized dye **PTZ-GLU** we adopted the Cu-assisted azide-alkyne cycloaddition (CuAAC) "click" reaction,[10,11] using the methyl 2,3,4-tri-*O*-acetyl-6-azido-6-deoxy-α-D-glucopyranoside, which was synthetized as reported in literature,[12] and the alkyne-functionalized dye **4**. The advantage of azide–alkyne cycloadditions is their high chemoselectivity, which makes these reactions particularly attractive to conjugate highly functional molecules as for example carbohydrates.[13] The triple bond has been introduced on the phenothiazine moiety through nucleophilic substitution in an analogous way as for **PTZ-TEG**, using NaH as base to deprotonate the nitrogen and propargyl bromide as alkylating reagent. Butynyl bromide has been tested as well for alkylation but the strong basic conditions precluded the achievement of the desired product because of likely side-reactions taking place on the butynyl chain. Anyway the presence of a sp^3 carbon on the propargyl chain guarantees that no π conjugation of the molecule with the triazole ring will be present in the dye. Click reaction has been performed in standard conditions using $CuSO_4$ as copper source and sodium ascorbate as reducing agent in a THF and water mixture. The thienyl group was introduced with a Suzuki-Miyaura cross-coupling, during such reaction step the basic conditions due to K_2CO_3 brought to the formation of the desired product with the simultaneous cleavage of the three acetate groups on the glucose. Such side reaction was not forecast but since the protecting groups were introduced to perform the previous steps there had been no problem in performing the final Knoevenagel condensation in basic conditions to afford the desired product.

Synthesis of PTZ-TEG and PTZ-GLU

General Procedure for Alkylation: Compound **1** (1 eq.) was dissolved in dry DMF under N_2 atmosphere, then the solution was cooled to 0°C using an ice bath and NaH 60% (2 eq.) was slowly added. After stirring at 0 °C for 1 h, the appropriate tosylate or bromide (2 eq.) was added and the solution was stirred at rt for 4 h, when TLC revealed the complete conversion of the starting material. The reaction mixture was quenched with iced water, then extracted with Et_2O and the organic phase was dried with Na_2SO_4 and concentrated. The crude was purified using flash column chromatography on silica gel.

General Procedure for Suzuki-Miyaura Cross-Coupling: Compound **2** or **5** (1 eq.) and Pd(dppf)Cl_2·CH_2Cl_2 (0.1 eq.) were dissolved in dimethoxyethane and stirred for 15 minutes under nitrogen atmosphere. Then 5-formyl-2-thienylboronic acid (2.4 eq.) and K_2CO_3 (10 eq.) were added as suspension in methanol. The reaction was performed with microwave irradiation (70 °C, 200 W, 90 minutes) and then quenched by pouring into a saturated solution of NH_4Cl. Filtration on Celite and extractions with organic solvent allowed to isolate the crude product, which was then purified through flash column chromatography on silica gel.

General Procedure for Knoevenagel Condensation: Compound **3** or **6** (1 eq.), cyanoacetic acid (10 eq.) and piperidine (10 eq. + catalytic) were dissolved in $CHCl_3$ and heated to reflux for 5 h. Then the solvent was evaporated and a solution of HCl 1 M (~50 mL) was added and the mixture was left under magnetic stirring for 5 h at rt. The dark red solid that precipitated was filtered and washed with water (3x30 mL) and petroleum ether (2x30 mL).

Compound **2** was synthetized according to general procedure for alkylation using product **1** (0.20 g, 0.56 mmol), NaH 60% (0.13 g, 1.12 mmol) and TEG-OTs (0.35 g, 1.12 mmol) in 5 mL of dry DMF. Extraction with Et_2O and purification with petroleum ether/AcOEt 5:1 as eluent, gave product **2** as pale yellow oil in 80% yield (0.70 g). ^{1}H NMR (500 MHz, $CDCl_3$) δ 7.21 (dd, *J* = 8.6, 2.2 Hz, 2H), 7.17 (d, *J* = 1.7 Hz, 2H), 6.73 (d, *J* = 8.7 Hz, 2H), 3.99 (t, *J* = 6.1 Hz, 2H), 3.78 (t, *J* = 6.1 Hz, 2H),

3.67 – 3.57 (m, 6H), 3.55 – 3.48 (m, 2H), 3.35 (s, 3H). ^{13}C NMR (126 MHz, $CDCl_3$) δ 143.7, 130.2, 129.6, 126.0, 116.6, 115.0, 71.9, 70.7, 70.6 (x3), 68.1, 59.0, 47.9.

Compound **3** was synthetized according to general procedure for Suzuki-Miyaura cross-coupling using product **2** (0.24 g, 0.48 mmol), Pd(dppf)Cl_2·CH_2Cl_2 (0.04 g, 0.05 mmol), 5-formyl-2-thienylboronic acid (0.21 g, 1.15 mmol), K_2CO_3 (0.66 g, 4.80 mmol), DME (5 mL) and methanol (5 mL). Extractions with AcOEt and purification with petroleum ether/AcOEt 2:1 as eluent, gave product **3** as an orange solid in 75 % yield (0.19 g). ^{1}H NMR (500 MHz, DMSO-d_6) δ 9.76 (s, 2H), 7.60 (d, *J* = 3.9 Hz, 2H), 7.31 (dd, *J* = 8.5, 2.1 Hz, 2H), 7.22 (d, *J* = 2.2 Hz, 2H), 7.19 (d, *J* = 3.9 Hz, 2H), 6.81 (d, *J* = 8.6 Hz, 2H), 3.99 (t, *J* = 6.0 Hz, 2H), 3.78 (t, *J* = 6.0 Hz, 2H), 3.71 – 3.51 (m, 6H), 3.50 – 3.45 (m, 2H), 3.29 (s, 3H). ^{13}C NMR (126 MHz, DMSO-d_6) δ 182.4, 152.7, 144.6, 141.6, 137.5, 127.8, 125.7, 124.6, 123.9, 123.2, 115.5, 71.8, 70.7, 70.5, 70.4(x2), 67.9, 58.9, 47.9.

Compound **4** was synthetized according to general procedure for alkylation using product **1** (0.20 g, 0.56 mmol), NaH 60% (0.13 g, 1.12 mmol), propargyl bromide (0.04 g, 1.12 mmol) in 5 mL of dry DMF. Extraction with Et_2O and purification with petroleum ether/AcOEt 20:1 as eluent, gave product **4** as pale yellow solid in 77% yield (0.17 g). ^{1}H NMR (400 MHz, $CDCl_3$) δ 7.28 (dd, *J* = 8.6, 2.2 Hz, 2H), 7.22 (d, *J* = 2.2 Hz, 2H), 7.04 (d, *J* = 8.6 Hz, 2H), 4.43 (d, *J* = 2.3 Hz, 2H), 2.47 (t, *J* = 2.3 Hz, 1H). ^{13}C NMR (101 MHz, $CDCl_3$) δ 143.1, 130.5, 129.5, 125.1, 116.1, 115.8, 78.2, 75.2, 38.8.

Compound **5** was synthetized by mixing compound **4** (0.12 g, 0.30 mmol) and methyl 2,3,4-tri-*O*-acetyl-6-azido-6-deoxy-α-D-glucopyranoside (0.09 g, 0.27 mmol) in THF (6 mL), and adding a second solution of $CuSO_4$·$5H_2O$ (0.08 g, 0.33 mmol) and sodium ascorbate (0.08 g, 0.41 mmol) in H_2O (2.5 mL), then the reaction mixture was stirred at rt in the dark for 4 h. TLC (petroleum ether/AcOEt 1:1) revealed the complete consumption of compound **4**, then the solvents were evaporated and the crude was dissolved in CH_2Cl_2 and washed with HCl 5% solution and brine. The crude was purified using flash chromatography (petroleum ether/AcOEt 8:2 then 4:6) affording compound **5** (0.19 g, 95%) as an oil. ^{1}H NMR (500 MHz, $CDCl_3$) δ 7.48 (s, 1H), 7.23 (d, *J* = 2.2 Hz, 2H), 7.15 (dd, *J* = 8.7, 2.3 Hz, 2H), 6.65 (d, *J* = 8.7 Hz, 2H), 5.42 (t, *J* = 10.0 Hz, 1H), 5.12 (s, 2H), 4.79 (d, *J* = 3.6 Hz, 1H), 4.67 – 4.58 (m, 2H), 4.51 (dd, *J* = 14.5, 2.1 Hz, 1H), 4.37 – 4.31 (m, 1H), 4.07 (td, *J* = 8.2, 4.1 Hz, 1H), 2.91 (s, 3H), 2.08 (s, 3H), 2.06 (s, 3H), 2.00 (s, 3H). ^{13}C NMR (101 MHz, $CDCl_3$) δ 170.1, 169.9, 169.7, 144.1, 143.2, 130.2, 129.6, 125.7, 123.8, 116.6, 115.5, 96.5, 70.6, 69.5, 69.4, 67.6, 55.2, 50.8, 44.6, 20.7 (x3).

Compound **6** was synthetized according to general procedure for Suzuki-Miyaura cross-coupling using product **5** (0.10 g, 0.13 mmol), Pd(dppf)Cl_2·CH_2Cl_2 (0.01 g, 0.01 mmol), 5-formyl-2-thienylboronic acid (0.05 g, 0.31 mmol), K_2CO_3 (0.18 g, 1.35 mmol), DME (3 mL) and methanol (3 mL). Extraction with AcOEt and purification with AcOEt/*i*PrOH 10:1 as eluent, gave product **6** as an orange solid in 74% yield (0.07 g). ^{1}H NMR (500 MHz, DMSO-d_6) δ 9.88 (s, 2H), 8.01 (d, *J* = 3.8 Hz, 2H), 7.97 (s, 1H), 7.69 (d, *J* = 3.6 Hz, 2H), 7.61 (s, 2H), 7.53 (d, *J* = 8.5 Hz, 2H), 7.02 (d, *J* = 8.6 Hz, 2H), 5.33 (d, *J* = 5.8 Hz, 1H), 5.24 (s, 2H), 4.93 (d, *J* = 4.7 Hz, 1H), 4.77 (d, *J* = 6.5 Hz, 1H), 4.71 (d, *J* = 14.0 Hz, 1H), 4.46 – 4.29 (m, 2H), 3.61 (t, *J* = 9.2 Hz, 1H), 3.23 – 3.11 (m, 1H), 3.02 – 2.93 (m, 1H), 2.73 (s, 3H). ^{1}H NMR (500 MHz, DMSO-d_6 + D_2O) δ 9.83 (s, 2H), 7.96 (d, *J* = 3.8 Hz, 2H), 7.92 (s, 1H), 7.61 (d, *J* = 3.8 Hz, 2H), 7.55 (s, 2H), 7.49 (d, *J* = 8.2 Hz, 2H), 6.99 (d, *J* = 8.6 Hz, 2H), 5.20 (s, 2H), 4.68 (d, *J* = 13.4 Hz, 1H), 4.35 (d, *J* = 3.6 Hz, 2H), 3.56 (s, 1H), 3.32 (s, 1H), 3.15 (dd, *J* = 9.5, 3.6 Hz, 1H), 2.97 (s, 1H), 2.70 (d, *J* = 24.2 Hz, 3H). ^{13}C NMR (126 MHz, DMSO-d_6) δ ^{13}C NMR (126 MHz, DMSO) δ 184.1, 152.0, 144.5, 143.1, 141.8, 139.8, 127.9, 126.3, 125.1, 124.6, 123.1, 116.7, 100.1, 73.5, 72.2, 72.2, 71.0, 54.4, 51.6, 44.5.

Compound **PTZ-TEG** was synthetized according to general for Knoevenagel condensation using product **3** (0.19 g, 0.34 mmol), cyanoacetic acid (0.29 g, 3.40 mmol), piperidine (0.34 g, 3.4 mmol) and $CHCl_3$ (6 mL). A dark red solid (0.22 g) has been isolated as the product in 92% yield. ^{1}H NMR (500 MHz, DMSO-d_6) δ 8.45 (s, 2H), 7.98 (d, *J* = 3.8 Hz, 2H), 7.71 (d, *J* = 3.8 Hz, 2H), 7.57 (m, 4H), 7.16 (d, *J* = 9.1 Hz, 2H), 4.13 (t, *J* = 5.3 Hz, 2H), 3.79 (t, *J* = 5.3 Hz, 2H), 3.66 – 3.43 (m, 6H), 3.43 – 3.29 (m, 2H), 3.20 (s, 3H). ^{13}C NMR (126 MHz, DMSO-d_6) δ 164.2, 152.0, 146.0, 145.0, 141.0, 134.5, 127.7, 126.5 125.0, 124.8, 123.8, 117.2, 116.9, 98.8, 71.7, 70.4, 70.2, 70.1, 67.8, 58.5, 44.1. HRMS (ESI) *m/z*: calcd. for $[M+H]^+$ $C_{35}H_{30}N_3O_7S_3$: 700.1246; found 700.0552; calcd. for $[M+Na]^+$ $C_{35}H_{29}N_3NaO_7S_3$: 722.1065; found 722.0307.

Compound **PTZ-GLU** was synthetized according to general for Knoevenagel condensation using product **6** (0.18 g, 0.27 mmol), cyanoacetic acid (0.11 g, 2.70 mmol), piperidine (0.22 g, 2.70 mmol) and $CHCl_3$ (5 mL). A dark red solid (0.19 g) has been isolated as the product in 90% yield. ^{1}H NMR (500 MHz, DMSO-d_6) δ 8.47 (s, 2H), 7.99 (m, 3H), 7.71 (d, *J* = 4.0 Hz, 2H), 7.57 (d, *J* = 2.1 Hz, 2H), 7.50 (dd, *J* = 8.5, 2.0 Hz, 2H), 7.05 (d, *J* = 8.7 Hz, 2H), 5.24 (s, 2H), 4.71 (d, *J* = 12.9 Hz, 1H), 4.46 – 4.29 (m, 2H), 3.61 (t, *J* = 9.5 Hz, 1H), 3.36 (t, *J* = 9.1 Hz, 1H), 3.17 (dd, *J* = 9.6, 3.6 Hz, 1H), 2.98 (t, *J* = 9.2 Hz, 1H), 2.74 (s, 3H). ^{13}C NMR (126 MHz, DMSO-d_6) δ 164.1, 152.2, 147.0, 144.6, 143.0, 142.0, 134.4, 127.7, 126.3, 125.1, 124.6, 123.1, 117.0, 116.8, 100.1, 98.2, 73.5, 72.2, 72.1, 71.0, 54.4, 51.6, 44.4. HRMS (ESI) *m/z*: calcd. for $[M+H]^+$ $C_{38}H_{31}N_6O_9S_3$: 811.1315; found 811.0627; calcd. for $[M+Na]^+$ $C_{38}H_{30}N_6NaO_9S_3$: 833.1134; found 833.0417

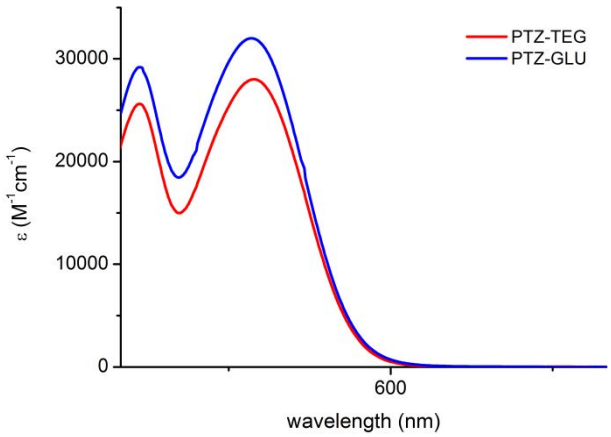

Figure S1. Absorption spectra of dyes **PTZ-TEG** and **PTZ-GLU** in THF

Table S1. Optical and electrochemical characterization of dye **PTZ-TEG** and **PTZ-GLU**.

Sample	λ_{max} [a] (nm)	ε ($M^{-1}cm^{-1}$)	V_{ox} (V vs. Fc) ± 10 mV	HOMO[b] eV ± 0.1 eV	V_{red} (V vs. Fc) ± 10 mV	LUMO[b] eV ± 0.1 eV
PTZ-TEG	470	28000 ± 1000	0.33	-5.5	-1.52	-3.7
PTZ-GLU	471	32000 ± 1000	0.30	-5.5	-1.49	-3.7

[a] Dye solution 10^{-5} M in THF. [b] Vacuum potential = Fc/Fc^+ + 5.2 V.

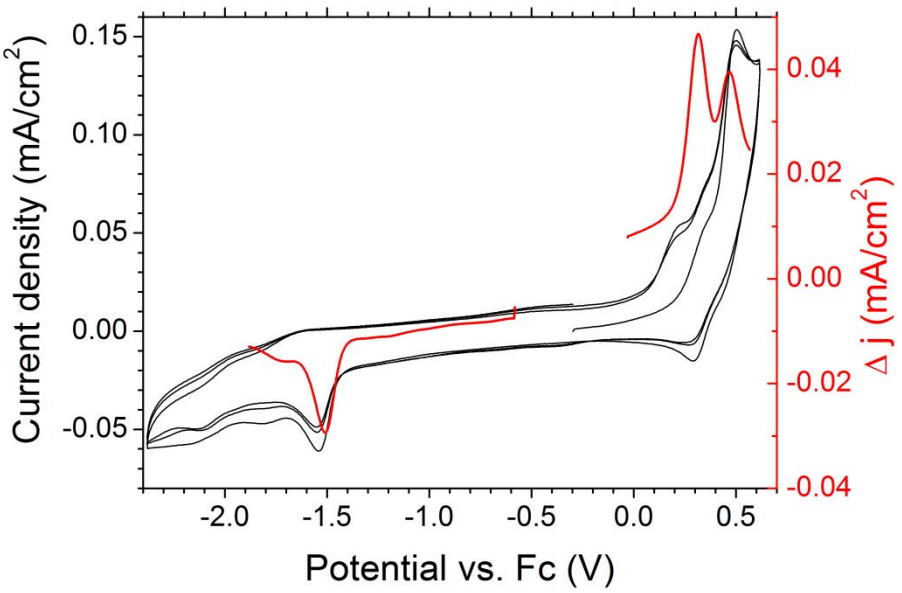

Figure S2. Electrochemistry of **PTZ-TEG:** CV (black line) and DPV (red line) measurements.

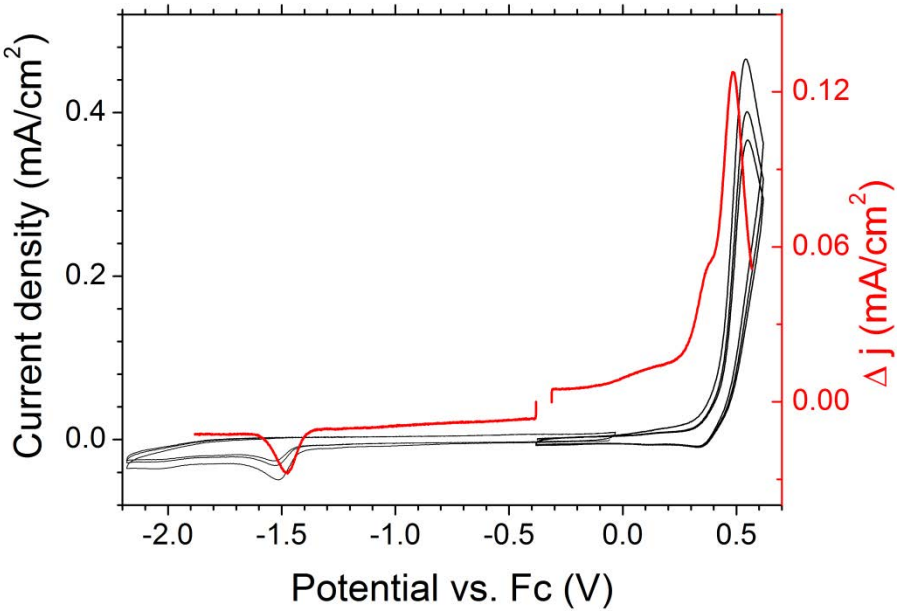

Figure S3. Electrochemistry of **PTZ-GLU:** CV (black line) and DPV (red line) measurements.

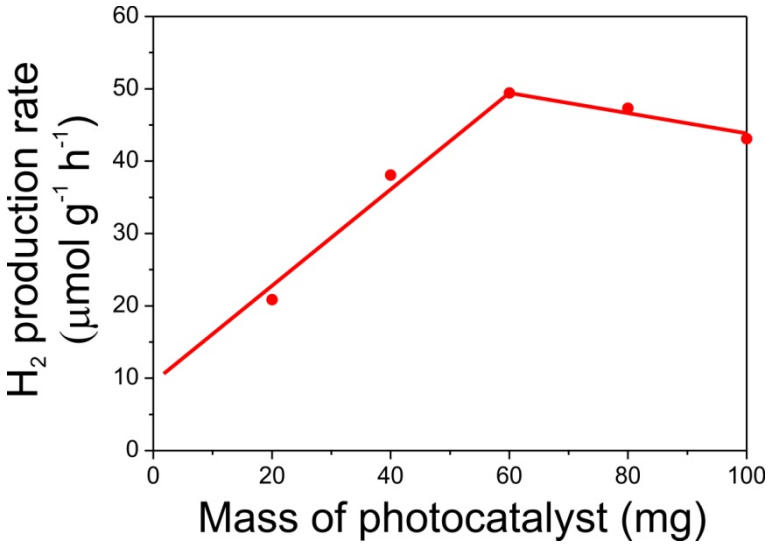

Figure S4. Optimization of the experimental conditions for photocatalytic H_2 production.

References

1. E. Bae, W. Choi, J. Park, H. S. Shin, S. B. Kim and J. S. Lee, *J. Phys. Chem. B*, 2004, **108**, 14093.
2. S.-H. Lee, Y. Park, K.-R. Wee, H.-J. Son, D. W. Cho, C. Pac, W. Choi and S. O. Kang, *Org. Lett.*, 2010, **12**, 460.
3. T. Montini, V. Gombac, L. Sordelli, J. J. Delgado, X. Chen, G. Adami and P. Fornasiero, *ChemCatChem*, 2011, **3**, 574.
4. I. Romero Ocaña, A. Beltram, J. J. Delgado Jaén, G. Adami, T. Montini and P. Fornasiero, *Inorg. Chim. Acta*, 2015, **431**, 197.
5. Sing, K. S. W.; Everett, D. H.; Haul, R. A. W.; Moscou, L.; Pierotti, R. A.; Rouquerol, J.; Siemieniewska, T. *Pure Appl. Chem.* 1985, **57**, 603.
6. B. Cecconi, N. Manfredi, R. Ruffo, T. Montini, I. Romero-Ocaña, P. Fornasiero and A. Abbotto, *ChemSusChem*, 2015, **8**, 4216.
7. H. Kisch and D. Bahnemann, *J. Phys. Chem. Lett.*, 2015, **6**, 1907.
8. H. Brunner and N. Gruber, *Inorg. Chim. Acta*, 2004, **357**, 4423.
9. M. Sailer, A. W. Franz and T. J. J. Müller, *Chem. Eur. J.*, 2008, **14**, 2602.
10. V. V. Rostovtsev, L. G. Green, V. V. Fokin and K. B. Sharpless, *Angew. Chem. Int. Ed.*, 2002, **41**, 2596.
11. C. W. Tornøe, C. Christensen and M. Meldal, *J. Org. Chem.*, 2002, **67**, 3057.
12. S. P. Chakrabarty, R. Ramapanicker, R. Mishra, S. Chandrasekaran and H. Balaram, *Biorg. Med. Chem.*, 2009, **17**, 8060.
13. A. J. Dirks, J. J. L. M. Cornelissen, F. L. van Delft, J. C. M. van Hest, R. J. M. Nolte, A. E. Rowan and F. P. J. T. Rutjes, *QSAR Comb. Sci.*, 2007, **26**, 1200.

^{1}H NMR and ^{13}C NMR spectra

Molecule 2

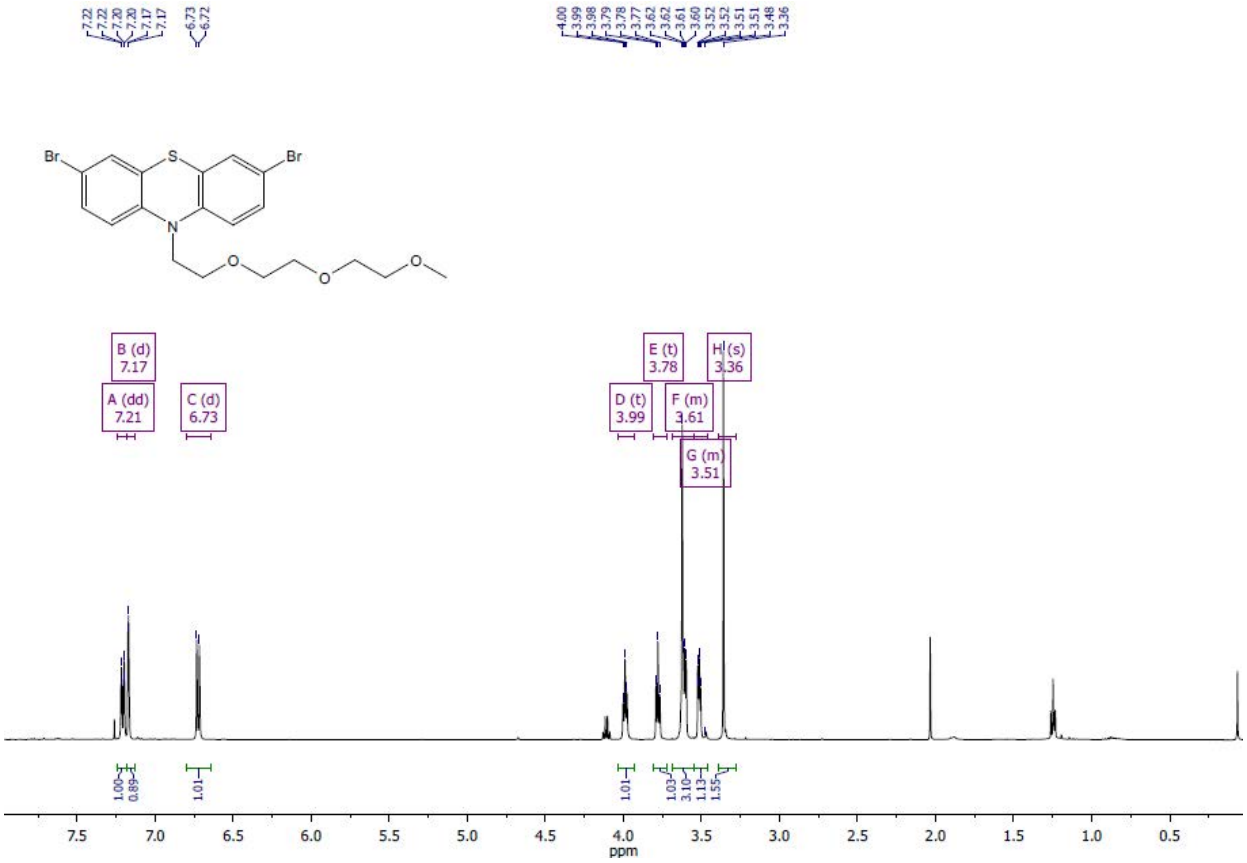

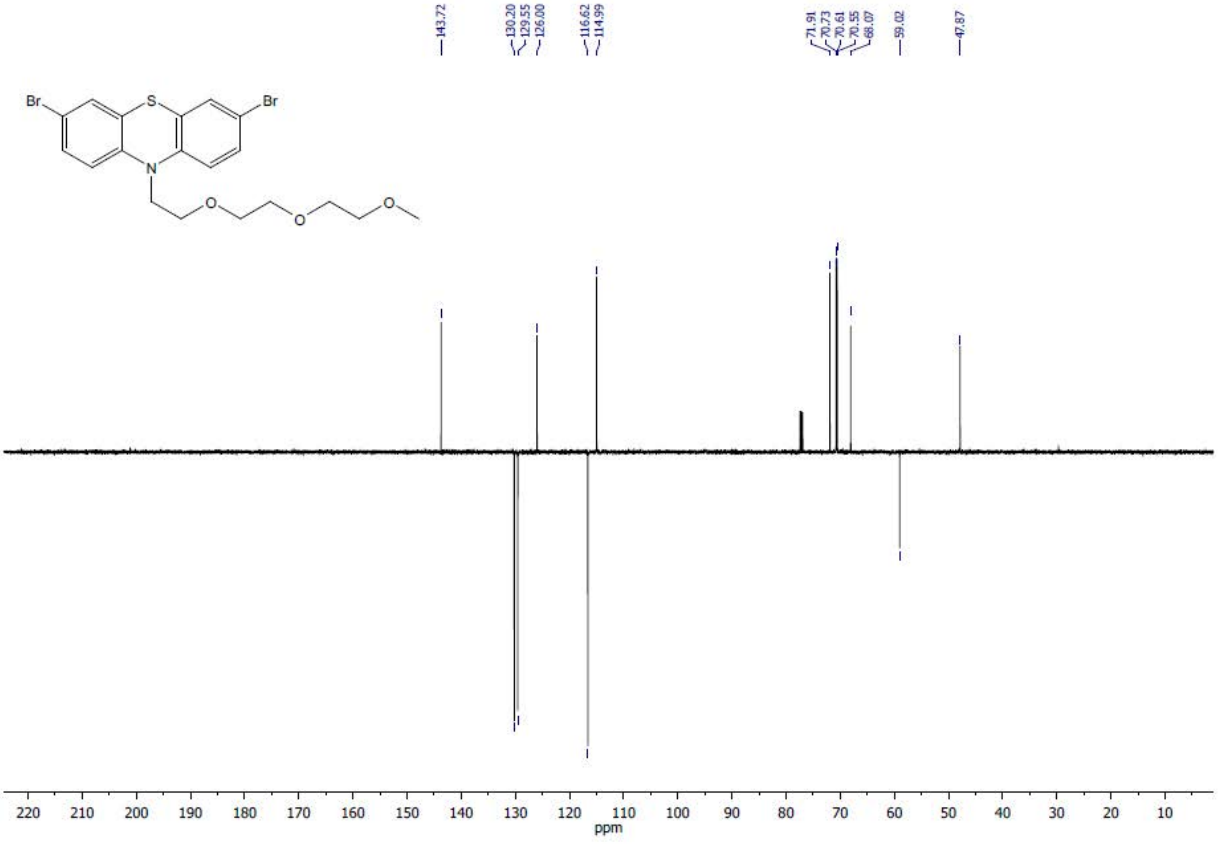

Molecule 3

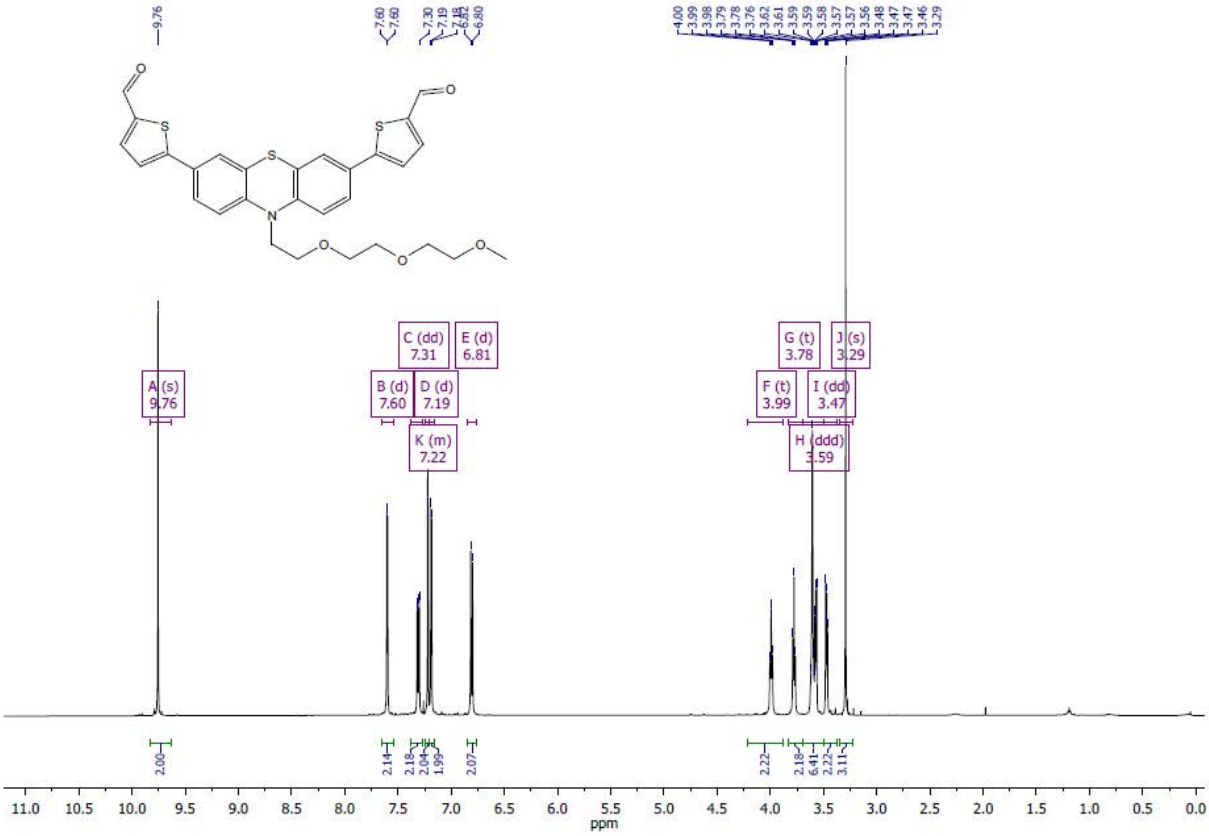
9.76
7.60
7.60
7.30
7.19
6.81
6.80
4.00
3.99
3.98
3.79
3.78
3.76
3.62
3.61
3.59
3.59
3.58
3.57
3.57
3.56
3.48
3.47
3.47
3.46
3.29
A (s) 9.76
B (d) 7.60
C (dd) 7.31
D (d) 7.19
E (d) 6.81
K (m) 7.22
F (t) 3.99
G (t) 3.78
H (ddd) 3.59
I (dd) 3.47
J (s) 3.29
2.00
2.14
2.18
2.04
1.99
2.07
2.22
2.18
6.41
2.22
3.11
ppm

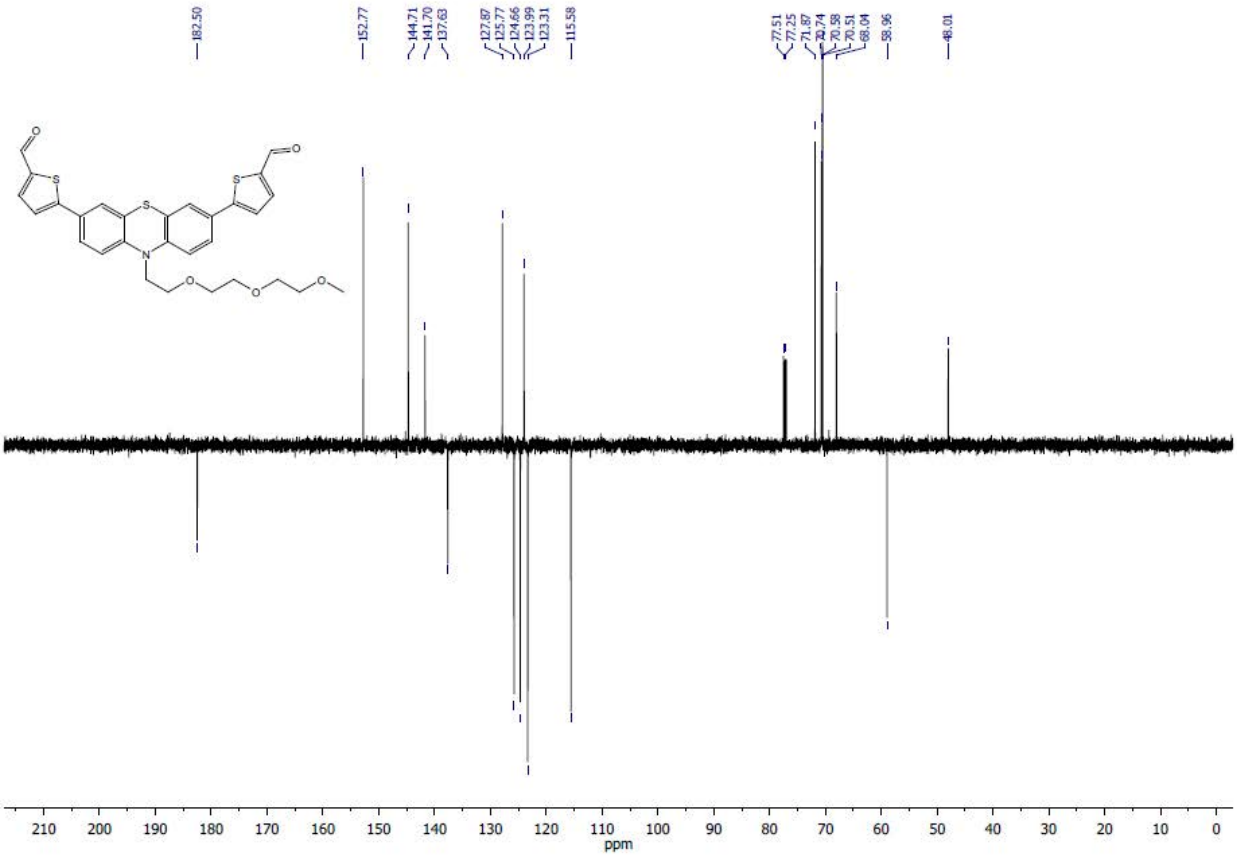
182.50
152.77
144.71
141.70
137.63
127.87
125.77
124.66
123.99
123.31
115.58
77.51
77.25
71.87
70.74
70.58
70.51
68.04
58.96
48.01
ppm

Molecule 4

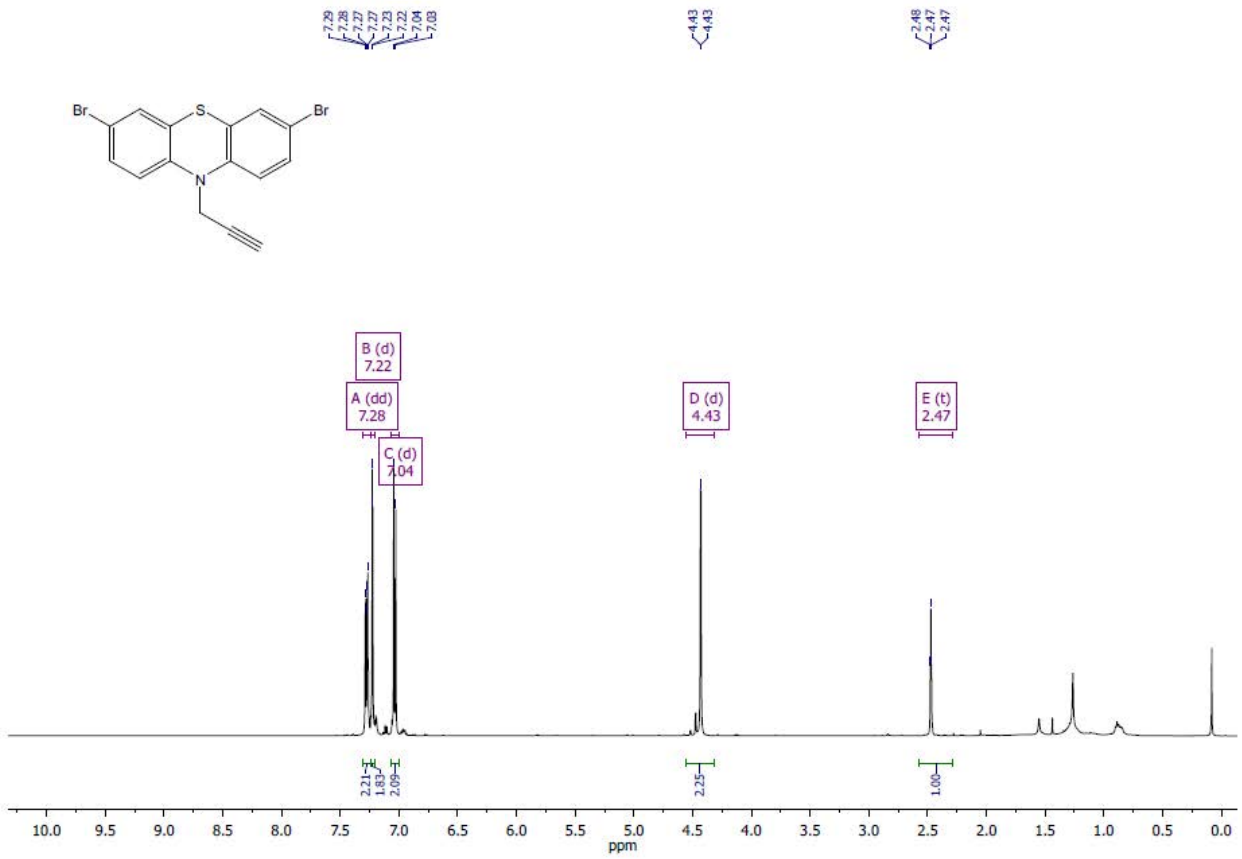
7.29
7.28
7.27
7.27
7.23
7.22
7.04
7.03
4.43
4.43
2.48
2.47
2.47
Br
S
Br
N
B (d)
7.22
A (dd)
7.28
C (d)
7.04
D (d)
4.43
E (t)
2.47
2.21
1.83
2.09
2.25
1.00
10.0 9.5 9.0 8.5 8.0 7.5 7.0 6.5 6.0 5.5 5.0 4.5 4.0 3.5 3.0 2.5 2.0 1.5 1.0 0.5 0.0
ppm

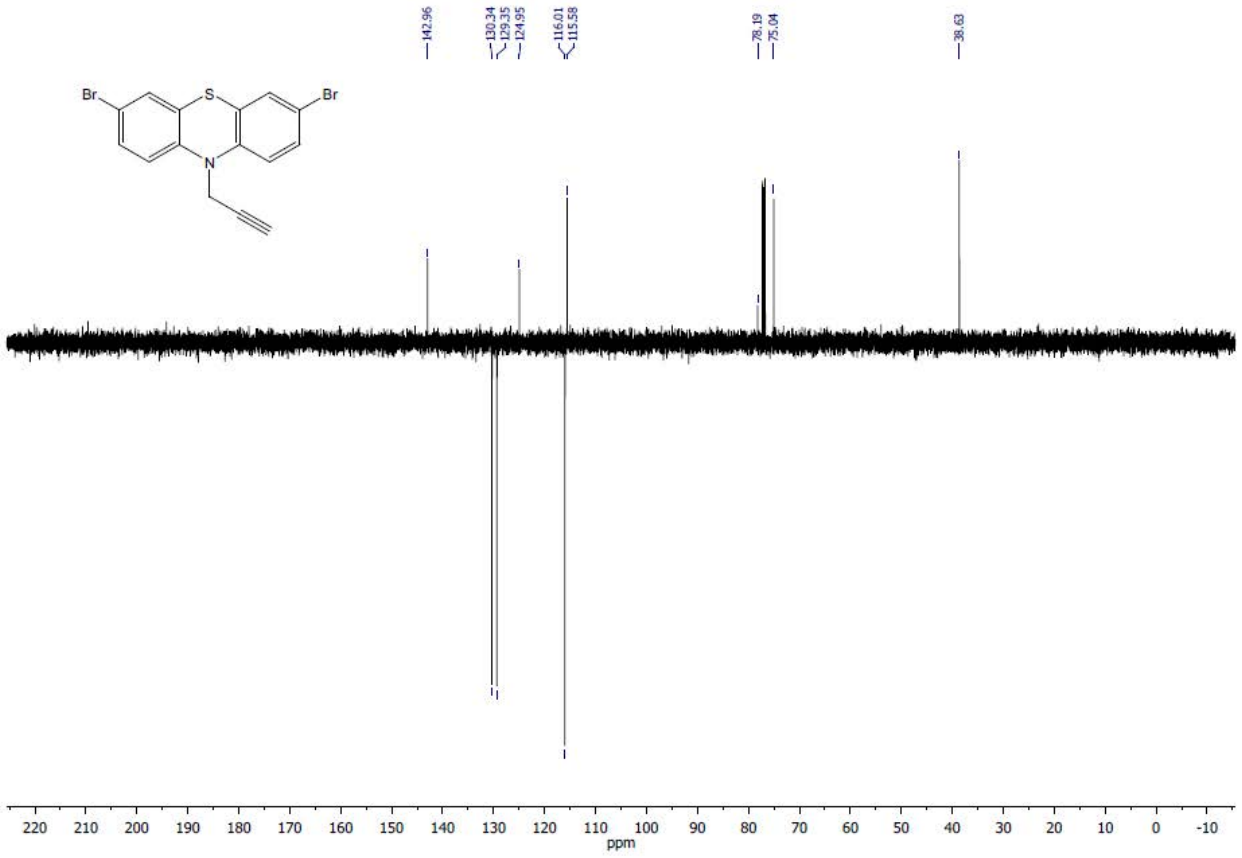
142.96
130.34
129.35
124.95
116.01
115.58
78.19
75.04
38.63
Br
S
Br
N
220 210 200 190 180 170 160 150 140 130 120 110 100 90 80 70 60 50 40 30 20 10 0 -10
ppm

Molecule 5

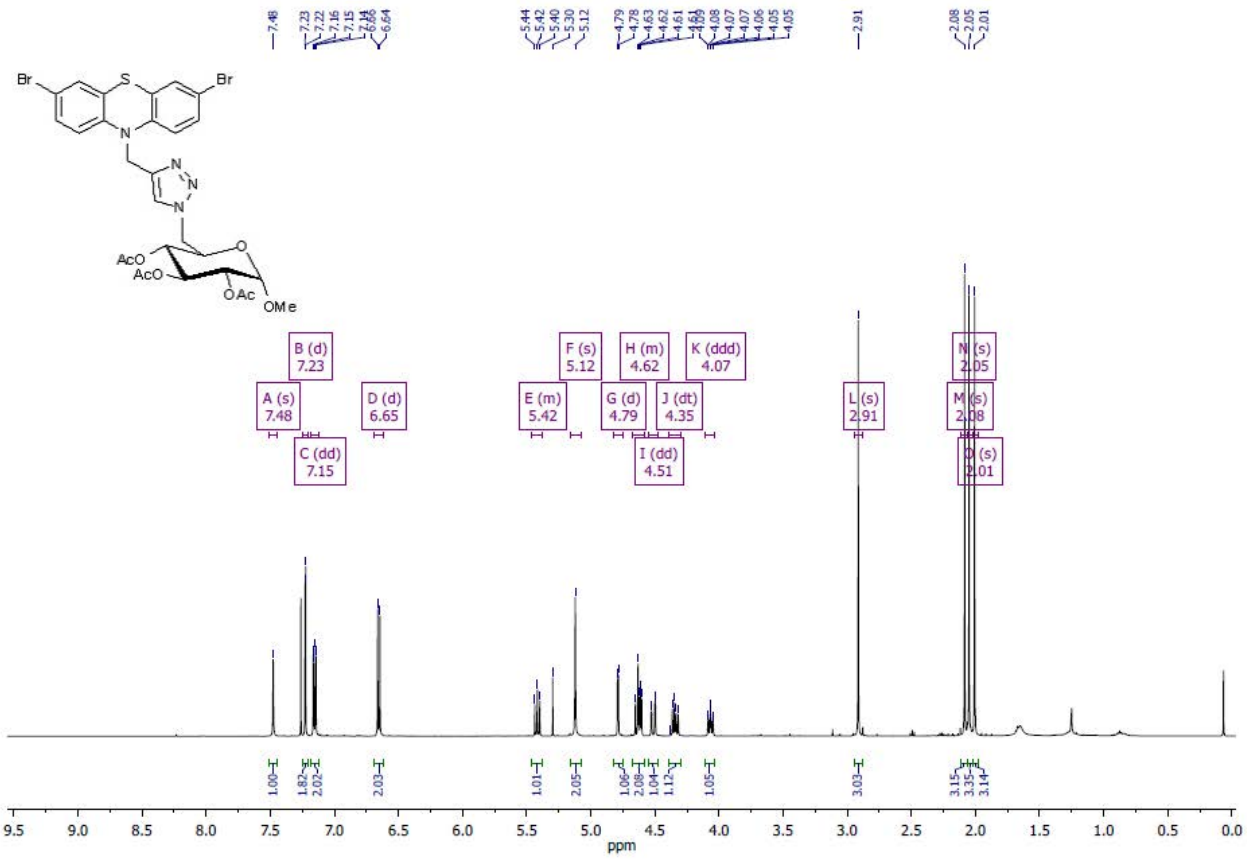
Br
S
Br
N
N
N
AcO
AcO
O
OAc
OMe
B (d) 7.23
A (s) 7.48
C (dd) 7.15
D (d) 6.65
F (s) 5.12
E (m) 5.42
H (m) 4.62
G (d) 4.79
K (ddd) 4.07
J (dt) 4.35
I (dd) 4.51
L (s) 2.91
N (s) 2.05
M (s) 2.08
O (s) 2.01
ppm

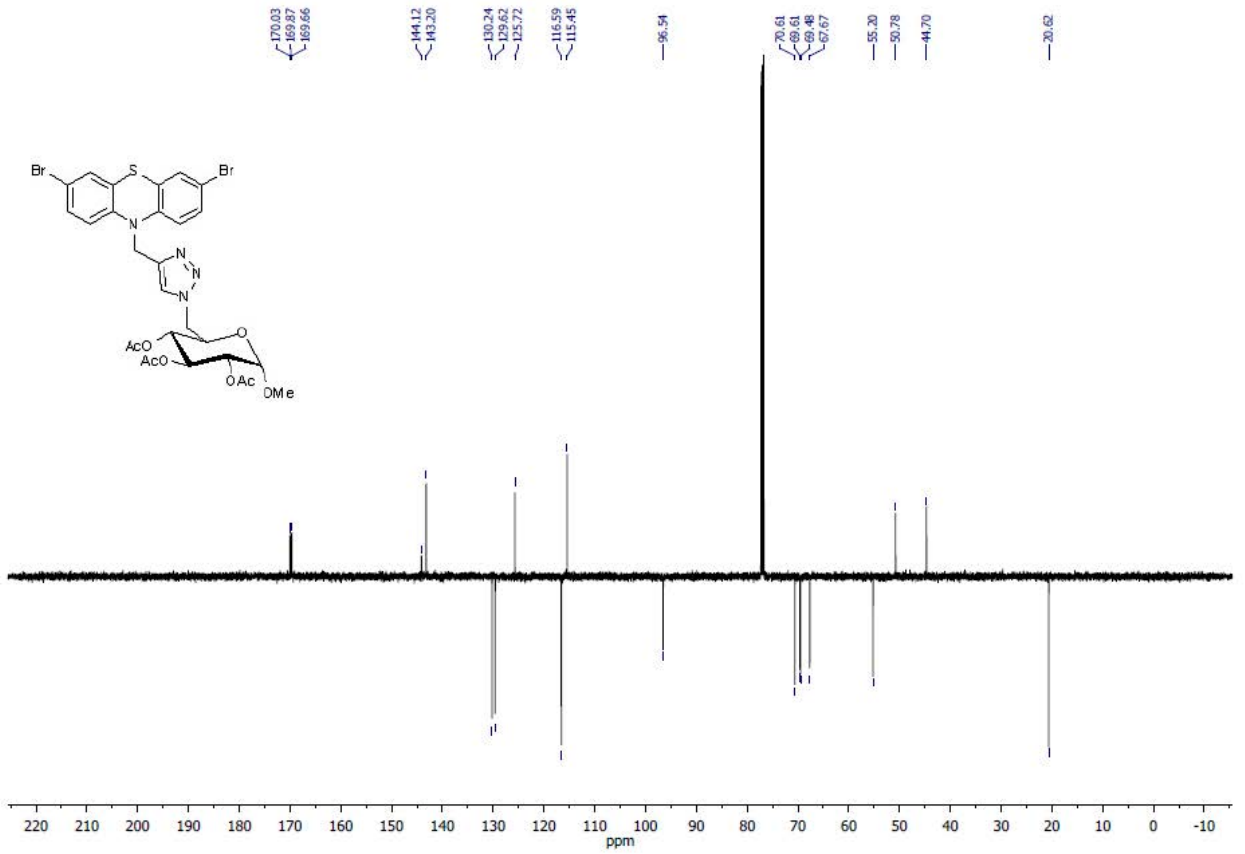
Br
S
Br
N
N
N
AcO
AcO
O
OAc
OMe
ppm

Molecule 6

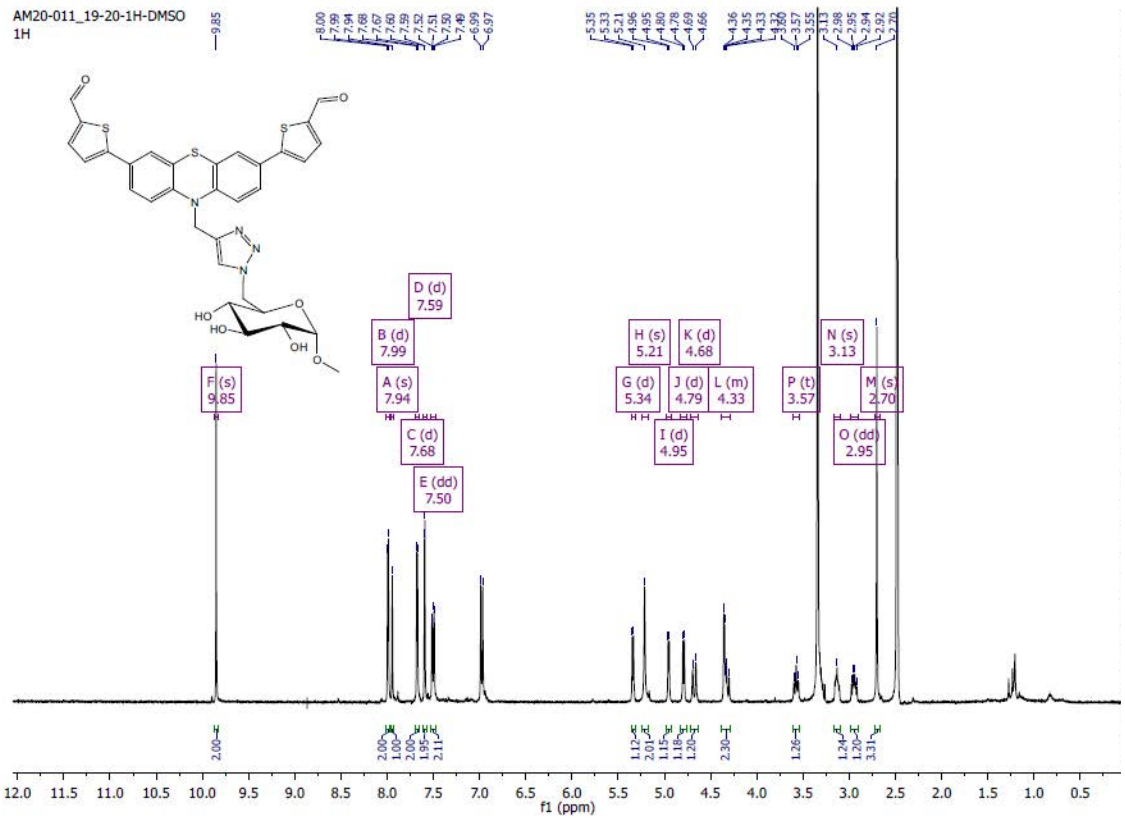

^{1}H NMR (DMSO + D_2O)

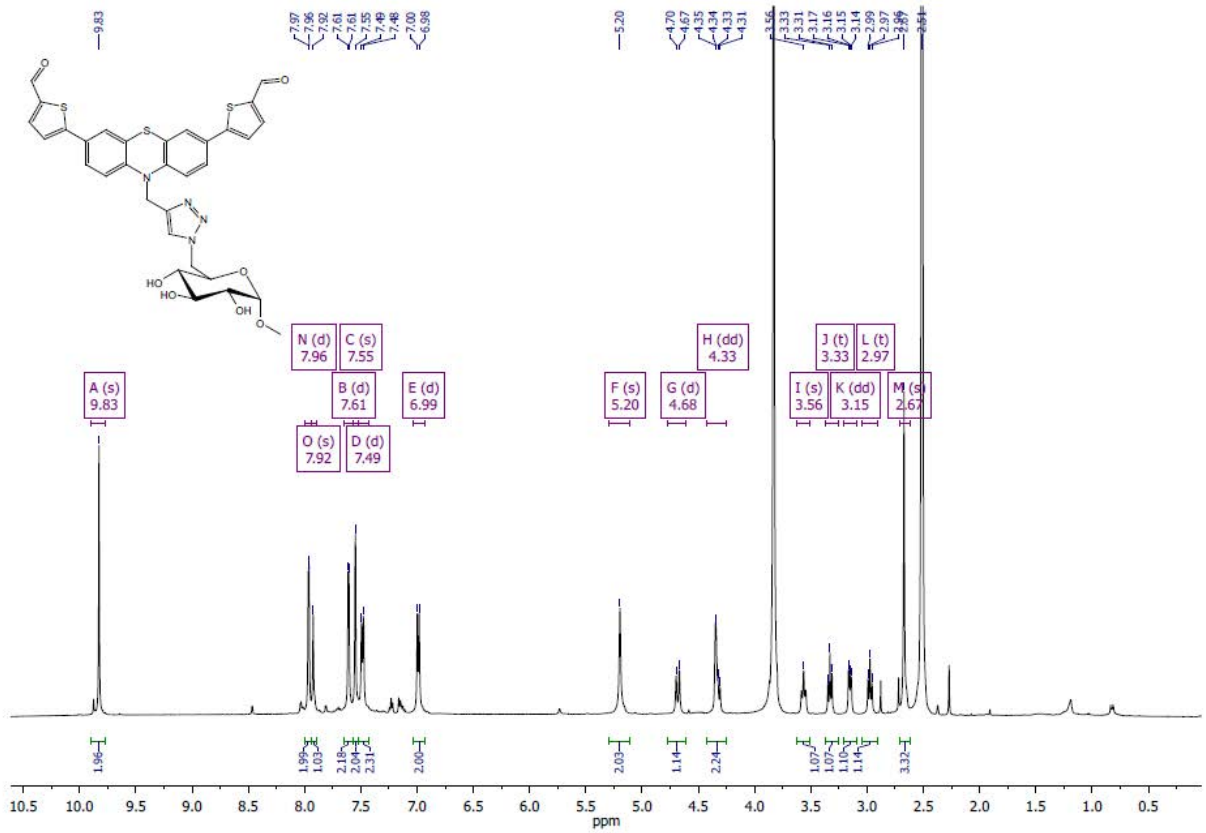

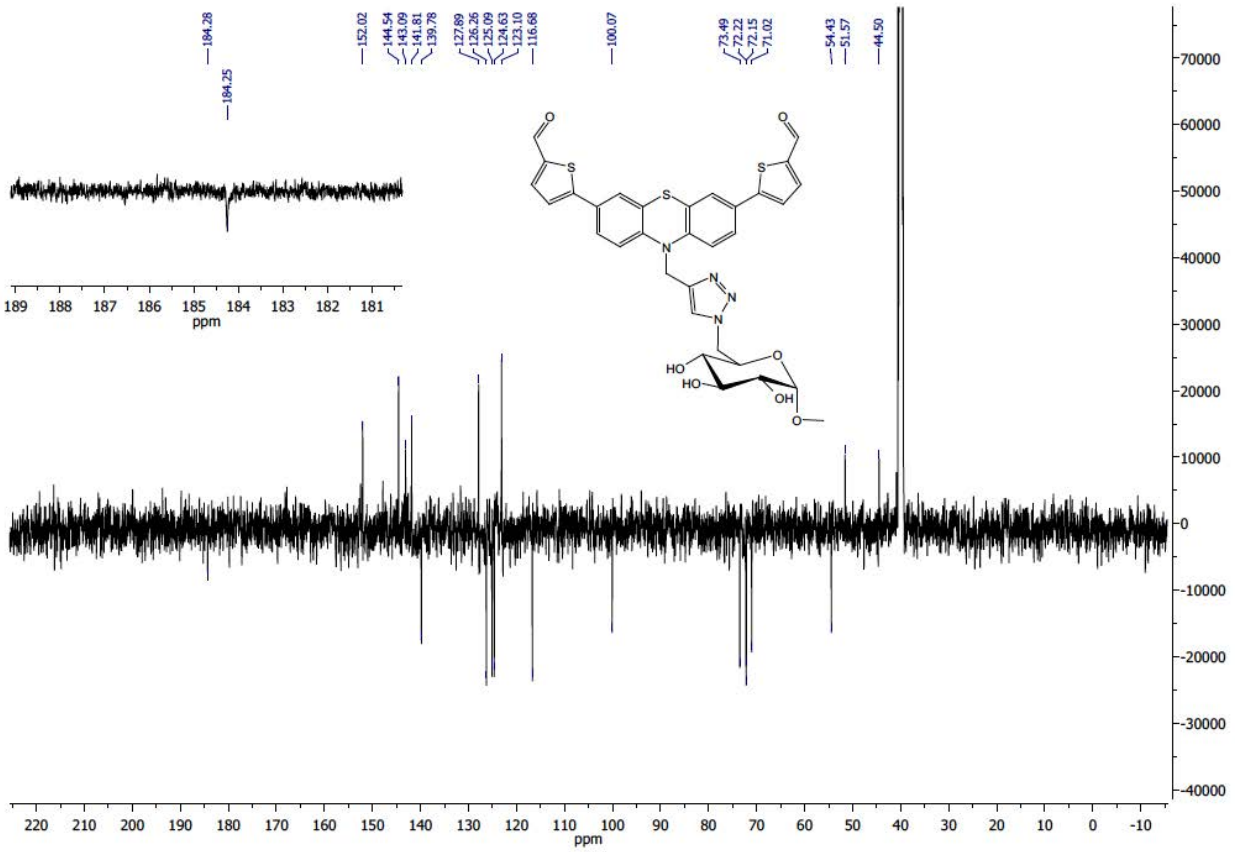
184.28
184.25
152.02
144.54
143.09
141.81
139.78
127.89
126.26
125.09
124.63
123.10
116.68
100.07
73.49
72.22
72.15
71.02
54.43
51.57
44.50
O
S
S
S
O
N
N
N
N
HO
HO
OH
O
O
189 188 187 186 185 184 183 182 181
ppm
70000
60000
50000
40000
30000
20000
10000
0
-10000
-20000
-30000
-40000
220 210 200 190 180 170 160 150 140 130 120 110 100 90 80 70 60 50 40 30 20 10 0 -10
ppm

PTZ-TEG

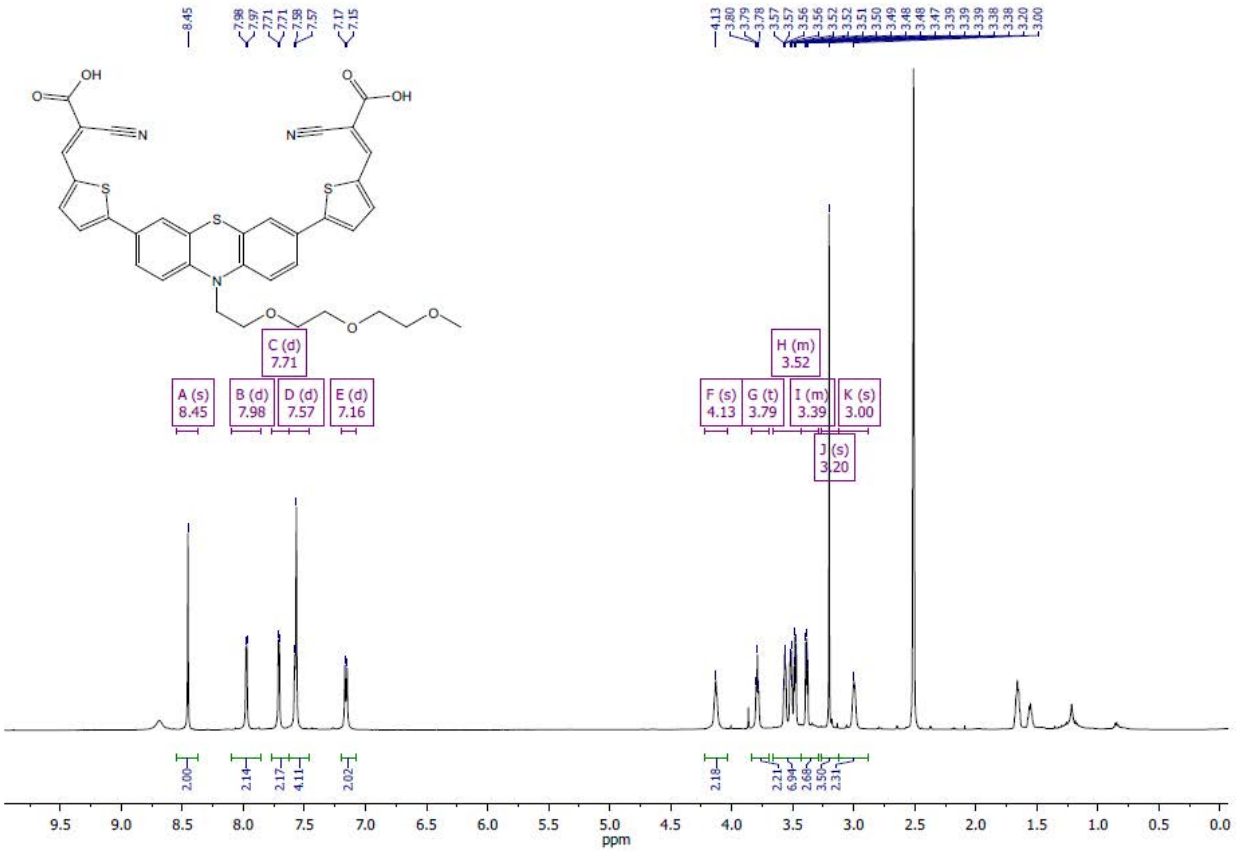
8.45
7.98
7.97
7.71
7.71
7.58
7.57
7.17
7.15
4.13
3.80
3.79
3.78
3.57
3.57
3.56
3.56
3.52
3.52
3.51
3.50
3.49
3.48
3.48
3.47
3.39
3.39
3.39
3.38
3.38
3.20
3.00
OH
O
N
S
O
O
O
O
C (d) 7.71
A (s) 8.45
B (d) 7.98
D (d) 7.57
E (d) 7.16
H (m) 3.52
F (s) 4.13
G (t) 3.79
I (m) 3.39
K (s) 3.00
J (s) 3.20
2.00
2.14
2.17
4.11
2.02
2.18
2.21
6.94
2.69
3.50
2.31
9.5 9.0 8.5 8.0 7.5 7.0 6.5 6.0 5.5 5.0 4.5 4.0 3.5 3.0 2.5 2.0 1.5 1.0 0.5 0.0
ppm

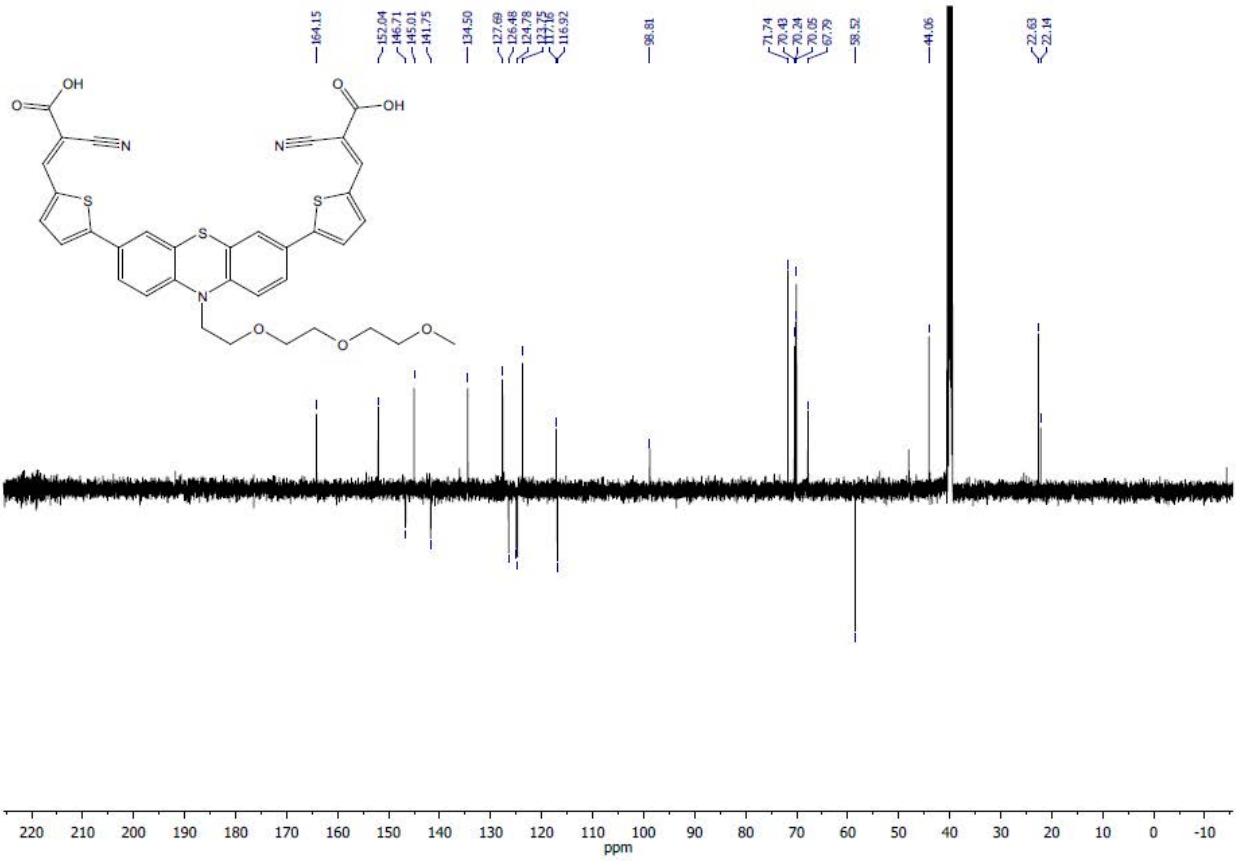
164.15
152.64
146.71
145.01
141.75
134.50
127.69
126.48
124.78
123.75
117.16
116.92
98.81
71.74
70.43
70.24
70.05
67.79
58.52
44.06
22.63
22.14
OH
O
N
S
O
O
O
O
220 210 200 190 180 170 160 150 140 130 120 110 100 90 80 70 60 50 40 30 20 10 0 -10
ppm

PTZ-GLU

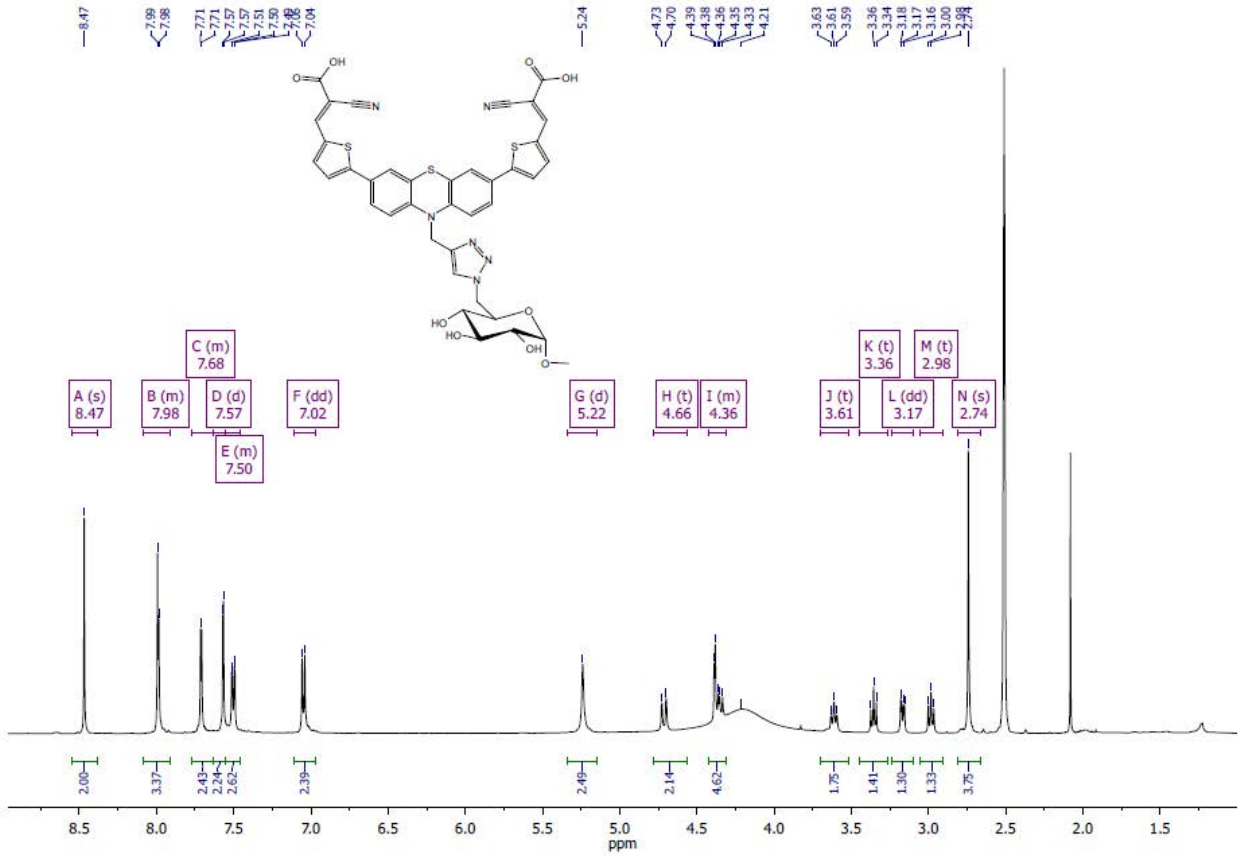
A (s) 8.47
B (m) 7.98
C (m) 7.68
D (d) 7.57
E (m) 7.50
F (dd) 7.02
G (d) 5.22
H (t) 4.66
I (m) 4.36
J (t) 3.61
K (t) 3.36
L (dd) 3.17
M (t) 2.98
N (s) 2.74
ppm

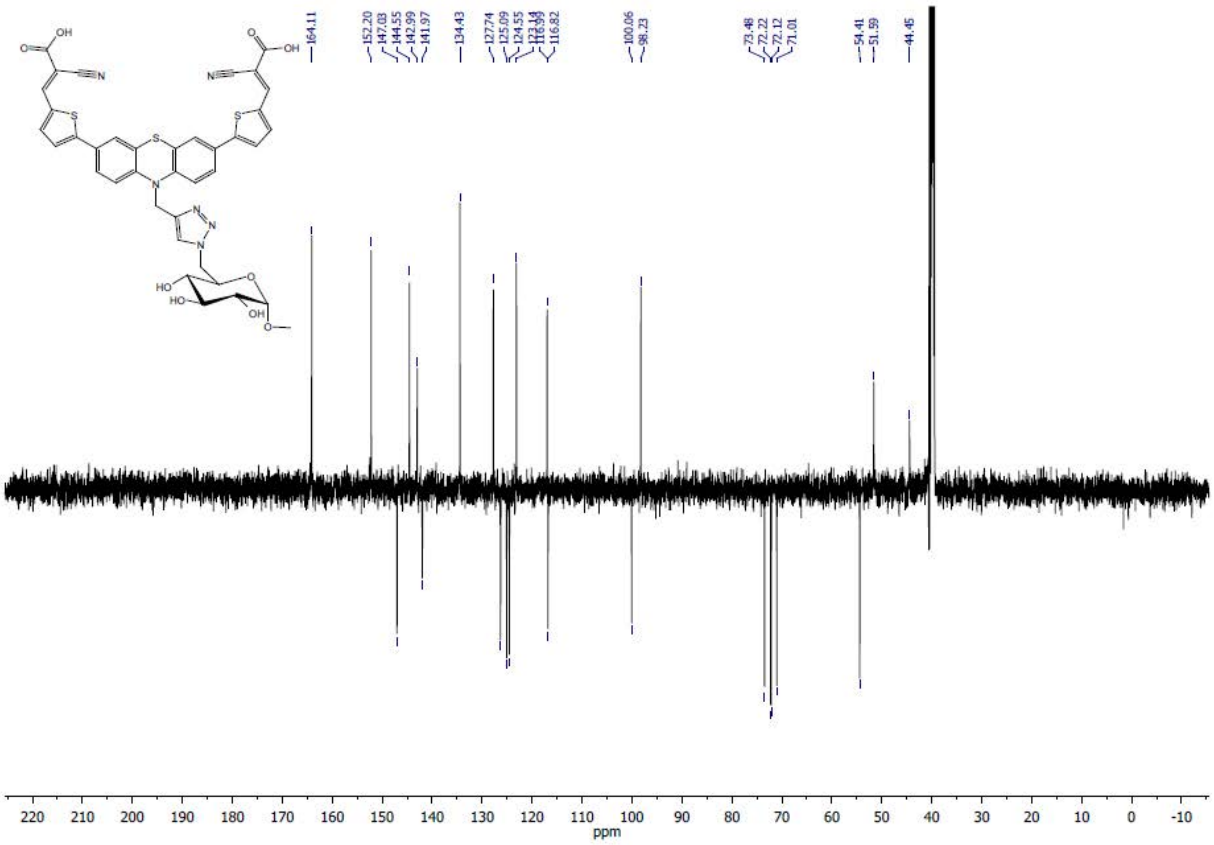
ppm